National Aeronautics and Space Administration
Contract No. NASw-6

External Publication No. 673

ACQUISITION AND TRACKING BEHAVIOR OF PHASE-LOCKED LOOPS

A. J. Viterbi

Copy No._____
pp. ii, 1-39

JET PROPULSION LABORATORY
California Institute of Technology
Pasadena 3, California

July 14, 1959

CONTENTS

Unclassified - FIGURES first line of text
Classified - Title or first line of text

FIGURES (Cont'd)

External Publication No. 673

ACQUISITION AND TRACKING BEHAVIOR OF PHASE-LOCKED LOOPS[1]

by A. J. Viterbi

I. INTRODUCTION

Phase-locked or APC loops have found increasing applications in recent years as tracking filters, synchronizing devices, and narrow-band FM discriminators. Considerable work has been performed to determine the noise-squelching properties of the loop when it is operating in or near phase lock and is functioning as a linear coherent detector (Refs. 1 and 2). However, insufficient consideration has been devoted to the non-linear behavior of the loop when it is out of lock and in the process of pulling in. Experimental evidence has indicated that there is a strong tendency for phase-locked loops to achieve lock under most circumstances. However, the analysis which has appeared in the literature (Refs. 3, 4, and 5) is limited to the acquisition of a constant frequency reference signal with only one phase-locked loop filter configuration.

This work represents an investigation of frequency acquisition properties of phase-locked loops for a variety of reference-signal behavior and loop configurations. Results are obtained concerning the frequency pull-in and tracking behavior (for both constant and linearly varying reference frequencies) of the following loop filter transfer functions:

---

[1]This paper presents the results of one phase of research carried out at the Jet Propulsion Laboratory, California Institute of Technology, under Contract No. NASw-6, sponsored by the National Aeronautics and Space Administration.

1. K (a wide-band amplifier or resistive pad)
2. $K\left[1 + a/p\right]$ (a single integration)
3. $K\left[(p + a)/(p + \alpha)\right]$ (a simple passive RC filter or imperfect integrator)
4. $K\left[1 + a/p + b/p^2\right]$ (a double integration)

The general approach involves solution of the non-linear differential equation which describes the system behavior, using analog and graphical methods. The terminology adopted in the text is the one in general use for closed-loop systems and servomechanisms. However, the application of phase-locked loops to the filtering of noisy signals has generated an alternate terminology in which the loop noise-bandwidth is the key parameter (Ref. 1). The results will be derived in terms of both sets of parameters and are summarized in Sec. IX.

II. BASIC OPERATION

Figure 1 represents the loop configuration. The frequency of the input reference signal, $\dot{\varphi}_s$, may be either constant or time varying. The frequency of the output of the voltage-controlled oscillator (VCO) consists of a constant equal to the center frequency of the oscillator, ω_c, plus a time-varying term proportional to the actuating signal. The VCO output is 90 deg out of phase with the input reference so that the multiplier output is proportional to the sum of two sinusoids of frequencies equal to the sum and difference of the two input frequencies.

Since the low-pass filter following the multiplier will not pass the sum frequency term, the multiplier output, e_d, is proportional to the sine of the difference phase, φ. The linear transfer function of the loop filter shall be termed $K_1F(p)$ where $F(0) = 1$ and operational notation is used throughout. Then

$$e_d = K_0 \sin \varphi = \frac{C_1C_2}{2} \sin \left[\varphi_s(t) - \omega_c t - \frac{K_0K_1K_2F(p)}{p} \sin \varphi\right] \qquad (1)$$

Clearly, the proportionality constant, K_0, is one-half the product of the input and return signal-amplitudes. Thus,

$$\sin \varphi = \sin \left[\varphi_s - \omega_c t - \frac{KF(p)}{p} \sin \varphi\right] \qquad (2)$$

where $K = K_0 K_1 K_2$ shall be defined as the loop gain. Differentiating the arguments of both sides of Eq. (2) yields

$$\dot{\varphi} + KF(p) \sin \varphi = \dot{\varphi}_s - \omega_c \qquad (3)$$

This then is the general equation for phase error of the phase-locked loop. At this point the following approximation is generally invoked:

$$\sin \varphi \simeq \varphi \text{ for } \varphi << 1 \text{ rad} \qquad (4)$$

which permits linear analysis to be performed and particularly the small-signal response of the system to noisy inputs to be considered. To determine the pull-in behavior of the loop, however, the non-linear Eq. (3) must be solved.

III. FIRST-ORDER LOOP WITH CONSTANT FREQUENCY INPUT

The first and most simple loop which shall be considered is one in which the loop filter has no energy storage elements and thus produces a constant transfer ratio (see Refs. 3 and 5). The reference input shall be a constant frequency sinusoid. Thus Eq. (3) becomes the first-order differential equation:

$$\dot{\varphi} = \Omega - K \sin \varphi \tag{5}$$

where

$$\Omega = \dot{\varphi}_s - \omega_c = \text{constant}$$

Figure 2 shows $\dot{\varphi}$ plotted against φ. If the VCO is initially at its center frequency, $\dot{\varphi}(0) = \Omega$ and $\varphi(0) = \pm n\pi$ (where n is an integer). If the frequency error $\dot{\varphi}$ is positive, the phase error φ tends to increase; for negative $\dot{\varphi}$, φ decreases. Hence, if n is an even integer and $\Omega < K$, the system will travel along the sinusoidal trajectory of Fig. 2 until it reaches the φ axis at $\varphi = \sin^{-1}(\Omega/K) + n\pi$. This is a stable point; $\dot{\varphi}$ can not become negative because φ would then tend to decrease and return the system to the φ axis. If n is an odd integer, the system will go through a larger part of the sinusoidal trajectory until it reaches a stable point at

$$(n + 1)\pi + \sin^{-1}\left(\frac{\Omega}{K}\right)$$

If $\Omega > K$, however, the trajectory never crosses the φ axis and a

stable or phase-lock point is never reached. Thus the pull-in frequency range of the loop is Ω_{max} = K rad/sec. For the first-order loop K is also equal to the closed-loop 3 db bandwidth.

When phase-lock does occur, the steady-state phase error is shown to be $\sin^{-1}(\Omega/K)$. The linear analysis which follows from the approximation (4) arrives at a steady-state error Ω/K, which is clearly an accurate estimate when $\Omega/K << 1$.

Pull-in time may also be determined from Eq. (5). Since $\dot{\varphi} = d\varphi/dt$, this can be rewritten as

$$\frac{dt}{d\varphi} = \frac{1}{\Omega - K \sin \varphi}$$

whence the pull-in time is given by

$$t = \int_{\varphi_{initial}}^{\varphi_{final}} \frac{d\varphi}{\Omega - K \sin \varphi} \qquad (6)$$

φ_{final} cannot be taken as $\sin^{-1}(\Omega/K) + n\pi$ since for this value the demoninator becomes zero and the integral becomes infinite. This is correct since, in fact, the time required to reach the steady state is infinite. To get a meaningful result φ_{final} can be taken as slightly less than the steady-state phase and the time required to reach it can be evaluated. The integral is expressed in terms of elementary functions in the standard tables.

The conclusions to be drawn regarding the first-order loop are that it will acquire lock within one cycle provided the initial

frequency error is less than the 3 db loop bandwidth and that the lock-in time is governed by the initial phase error.

IV. SECOND-ORDER LOOP WITH CONSTANT FREQUENCY INPUT

To overcome the limited pull-in range of the first order loop, and to provide for tracking linearly varying frequencies with narrow bandwidths, an integrator is generally used in the loop filter. Then

$$F(p) = 1 + \frac{a}{p} \tag{7}$$

and Eq. (3) becomes

$$p\varphi + \frac{Kp + aK}{p} (\sin \varphi) = \Omega \tag{8}$$

Letting $aK = \omega_n^2$ and $K = 2\zeta \omega_n$ and differentiating, the second-order differential equation which results is

$$p^2\varphi + 2\zeta \omega_n p (\sin \varphi) + \omega_n^2 \sin \varphi = 0 \tag{9}$$

The characteristic polynominal when the equation is linearized by approximation (4) becomes

$$p^2 + 2\zeta \omega_n p + \omega_n^2 = 0 \tag{10}$$

In servo terminology ω_n is the undamped natural frequency and ζ the damping factor for the linearized servo loop.

Rewriting Eq. (9) without operational notation:

$$\frac{d^2\varphi}{dt^2} + 2\zeta\,\omega_n \cos\varphi\,\frac{d\varphi}{dt} + \omega_n{}^2 \sin\varphi = 0 \qquad (11)$$

Making the substitution

$$t = \frac{\tau}{2\zeta\,\omega_n} \qquad (12)$$

$$4\zeta^2\,\omega_n{}^2\,\frac{d^2\varphi}{d\tau^2} + 4\zeta^2\,\omega_n{}^2 \cos\varphi\,\frac{d\varphi}{d\tau} + \omega_n{}^2 \sin\varphi = 0 \qquad (13)$$

Normalizing and letting

$$\frac{d\varphi}{d\tau} = \dot{\varphi} = \frac{1}{2\zeta\,\omega_n}\,\frac{d\varphi}{dt} \qquad (14)$$

$$\ddot{\varphi} + \dot{\varphi}\cos\varphi + \frac{1}{4\zeta^2}\sin\varphi = 0 \qquad (15)$$

Thus one of the parameters has been eliminated by normalizing the time parameter. It would now be of interest to construct a plot of $\dot{\varphi}$ as a function of φ as was done in the previous Section. To this aim let $\varphi = x$ (the abscissa) and $\dot{\varphi} = y$ (the ordinate). This requires that $y = \dot{x}$ and $\ddot{\varphi} = \dot{y}$. Then Eq. (15) becomes

$$\dot{y} + y\cos x + \frac{\sin x}{4\zeta^2} = 0$$

or

$$\frac{\dot{y}}{y} = \frac{\dot{y}}{\dot{x}} = \frac{dy}{dx} = -\cos x - \frac{\sin x}{4\zeta^2 y} \tag{16}$$

which relates the slope of the system trajectories to the instantaneous frequency and phase errors and permits their plotting. Certain observations can be made based on Eq. (16):

1. For large y (which corresponds to large frequency error) the second term on the right becomes small and the trajectories become nearly sinusoidal.
2. For $x = 0$ ($\varphi = 0$), the slope is always - 1. Hence the y axis is the - 1 isocline (line of constant slope). The overall pattern can be determined by finding other isoclines which in general will not be straight lines.
3. The equation is periodic in x with period 2π; that is, the slope of the trajectories is the same at (x_0, y_0) as it is at $(x_0 + 2n\pi, y_0)$. Hence, to describe the behavior it is only necessary to plot the trajectories for $-\pi < x < \pi$.
4. At $y = 0$, $x = \pm n\pi$ (n an integer or zero) the slope dy/dx is indeterminate since the second term on the right becomes 0/0. These points are called singularities and are either stable points of the system or centers of instability as will be discussed more fully below.

The graphical procedure just described for finding solutions of the non-linear differential Eq. (15) is the so-called "phase-plane" method (Refs. 6 and 7). The procedure of determining the isoclines

and sketching the various trajectories is a long and tedious process, however. On the other hand, Eq. (15) is easily programmed for an analog computer as is shown in the simplified diagram of Fig. 3. The voltage representing φ is used to actuate the x axis of a plotter and that representing $\dot{\phi}$ goes to the y axis.

This results in the plots of Figs. 4 through 7 for various values of ζ. The φ = x axis extends from $-\pi$ to $+\pi$. The following observations may be made from the figures:

1. For large values of y (positive and negative) the trajectories are practically sinusoids. The trajectories are traversed from left to right in the upper half plane and vice versa in the lower. For large positive y a small decay may be noted as the trajectory traverses the strip from $\varphi = -\pi$ and $\varphi = \pi$. The rate of decay becomes greater as y decreases. Since the behavior is periodic in each strip of width, 2π, the decay will continue and increase in each successive strip until at $x = \varphi = n\pi$ (where n is some odd integer) the value of y will be below the line A - A. At this point the system will stop skipping cycles and the phase and frequency error will decay in toward $\dot{\varphi} = 0$, $\varphi = (n + 1)\pi$ and phase-lock will have been achieved. The same behavior ensues when the initial frequency error is negative except that the movement of the trajectories is from right to left. The system may be said to be in frequency-lock when the errors lie within the lines

A - A in a particular strip since when this condition exists the loop stops skipping cycles.

2. The singular points at $x = \pm n\pi$ ($n = 0, 1, 2, \ldots$) are indeed points of stability or centers of instability as mentioned above. When n is even there are stable points where the loop achieves phase-lock. These are called nodes or foci depending upon whether the system is overdamped (Fig. 4) or underdamped (Figs. 6 and 7). At odd multiples of π there is a center of instability known as a saddle point. Near this point, no matter what the direction of the trajectories may be, the magnitude of the frequency error will decrease until the saddle point is almost reached and then quickly increase again. Further properties of the singular points may be found in Refs. 6 and 7 on phase-plane techniques, but these are not necessary for the discussion.

3. It can be seen by comparing the value of y for which the line A - A crosses the point $x = -\pi$ on the various figures that the region of frequency-lock is extended as ζ decreases. This, however, is a consequence of the normalization of Eq. (12). Letting the true radian frequency $d\varphi/dt = \omega$ rad/sec, and using Eq. (14) there results

$$\omega = 2\zeta\, \omega_n\, \dot{\varphi} = 2\zeta\, \omega_n y \qquad (17)$$

Figure 8 is a plot of the limiting value y and ω/ω_n

for frequency-lock as a function of ζ obtained using the analog computer. Clearly, the more damped the system the wider is the region of frequency-lock for a given loop natural frequency.

The qualitative intuition obtained by examining the phase-plane plots may be put on a somewhat more quantitative basis. First, it will be shown that the pull-in range is theoretically infinite. Then approximate expressions will be derived for the frequency error decay per cycle and the pull-in time.

If both sides of Eq. (16) are multiplied by y and integrated between the limits $-\pi$ and $+\pi$ the result is

$$\frac{1}{2}\left[y^2(\pi) - y^2(-\pi)\right] = -\int_{-\pi}^{\pi} y \cos x \, dx - \frac{1}{4\zeta^2}\int_{-\pi}^{\pi} \sin x \, dx \qquad (18)$$

The second term on the right is zero while the first may be integrated by parts to yield:

$$\frac{1}{2}\left[y^2(\pi) - y^2(-\pi)\right] = \int_{-\pi}^{\pi} \sin x \, dy \qquad (19)$$

If the expression for dy from Eq. (16) is substituted into Eq. (19) there results:

$$\frac{1}{2}\left[y^2(\pi) - y^2(-\pi)\right] = -\int_{-\pi}^{\pi} \sin x \cos x \, dx - \frac{1}{4\zeta^2}\int_{-\pi}^{\pi} \frac{\sin^2 x}{y} \, dx \qquad (20)$$

The first term is clearly zero and the second can be rewritten as

$$\frac{1}{2}\left[y^2(\pi) - y^2(-\pi)\right] = -\frac{1}{8\zeta^2}\int_{-\pi}^{\pi}\frac{1-\cos 2x}{y}\,dx \qquad (21)$$

Clearly, for positive y the integrand is positive for all values of x between the limits $\pm\pi$, making the right side of Eq. (21) negative. Therefore, during each cycle of width 2π, the value of y must decrease for all initial values of y, which implies that the pull-in range is infinite when a perfect integrator is used in the loop filter.

To determine approximately the decrease in y per cycle of x it may be assumed that for y above the line A - A the rate of decrease per cycle is constant. This approximation is, of course, best for large y. Then,

$$y(x) = y(-\pi) - \sin x - \beta x \qquad (22)$$

for $-\pi < x < \pi$ where $\beta = \delta y/2\pi$ and δy is the decrease per cycle.

Substitution into Eq. (16) yields

$$\frac{dy}{dx} = -\cos x - \frac{\sin x}{4\zeta^2\, y(-\pi)\left[1 - \frac{\sin x}{y(-\pi)} - \frac{\beta x}{(y(-\pi)}\right]}$$

If $y(-\pi) >> 1$

$$-\delta y = y(\pi) - y(-\pi) \cong \frac{-1}{4\zeta^2\, y(-\pi)}\int_{-\pi}^{\pi}\left(\sin x + \frac{\sin^2 x}{y(-\pi)} + \frac{\beta\, x \sin x}{y(-\pi)}\right)dx$$

Substituting Eq. (22) for y, assuming $y(-\pi) >> 1$ and $\beta << 1$, and preserving only the first and second order terms of the expansion yields:

$$\delta t \simeq \frac{1}{2\zeta\ \omega_n\ y(-\pi)} \int_{-\pi}^{\pi} \left[1 + \frac{\sin x}{y(-\pi)} + \frac{\sin^2 x}{y^2(-\pi)}\right] dx$$

$$\simeq \frac{\pi}{2\zeta\ \omega_n} \left[\frac{2}{y(-\pi)} + \frac{1}{y^3(-\pi)}\right] \tag{26}$$

If δy is small (which is certainly the case for $y > 3$) the ratio $\delta t/\delta y$ is a good estimate of the derivative of decay time with respect to the magnitude of frequency error. Dividing Eq. (26) by Eq. (23) yields:

$$\frac{dt}{dy} \simeq \frac{2\zeta}{\omega_n} \left[2y - \frac{1}{y} - \frac{1}{y^3}\right] \tag{27}$$

Integrating between the limits y_0, the initial error, and y_A, the value at the line A - A,

$$t \simeq \frac{2\zeta}{\omega_n} \left[y_0^2 - y_A^2 - \ln\left(\frac{y_0}{y_A}\right) + \frac{1}{2y_0^2} - \frac{1}{2y_A^2}\right] \tag{28}$$

is an approximation of the time required for frequency-lock when the initial frequency error is $\Omega_0 = 2\zeta\ \omega_n y_0$ rad/sec. Of course, the derivative approximation becomes increasingly crude as y approaches

Evaluation of the integral yields

$$\delta y = \frac{\pi(1 + 2\beta)}{4\zeta^2 \, y^2(-\pi)}$$

Substituting for β from Eq. (22):

$$\delta y = \frac{\pi}{4\zeta^2 \left[y^2(-\pi) - 1\right]} \tag{23}$$

This expression checks rather well with analog results down to $y(-\pi) = 3$.

By similar methods an expression may be obtained for the time required to achieve frequency-lock (defined as the point at which the trajectory dips below the line A - A). Since

$$y = \dot{\varphi} = \frac{d\varphi}{d\tau} = \frac{dx}{d\tau}$$

or

$$\tau = \int \frac{dx}{y} \tag{24}$$

using Eq. (12) the time per cycle is:

$$\delta t = \frac{\delta\tau}{2\zeta \, \omega_n} = \frac{1}{2\zeta \, \omega_n} \int_{-\pi}^{\pi} \frac{dx}{y} \tag{25}$$

y_A. However, if y_0 was large to begin with, terms of Eq. (28) are small with respect to the first, and asymptotically the pull-in time will be:

$$t \simeq \frac{2\zeta\, y_0^2}{\omega_n} = \frac{\Omega_0^2}{2\zeta\, \omega_n^3} \text{ seconds} \qquad (29)$$

It should be noted that if the integrator in the loop filter is not perfect the pull-in range of the loop is no longer infinite, but is proportional to the finite time constant of the filter. This will be shown in a later section.

V. SECOND-ORDER LOOP WITH LINEARLY VARYING FREQUENCY INPUT

When a phase-locked loop is used as a tracking filter or FM discriminator it has to follow an input reference with variable frequency. If this variation is due to a doppler shift it will be almost linear over a large part of the tracking period. If it is due to frequency modulation the maximum slope of the modulation will be limited by its bandwidth. It follows that a loop which can follow a frequency which varies linearly at this maximum rate can certainly follow the modulation.

The input frequency to be considered is then $\omega_s + Dt$. For a second-order loop the general Eq. (3) becomes:

$$p\varphi + \frac{Kp + aK}{p} (\sin \varphi) = \Omega + Dt \qquad (30)$$

where Ω is the initial frequency error which may be zero if the loop was originally in lock when the linear variation Dt of the input began. Since the right-hand side of Eq. (30) is the difference between the reference and VCO frequencies, the time-varying frequency may just as well be that of the VCO, corresponding to a constant drift of the oscillator. Following precisely the development and substitution of Eq. (8) through (15) of the previous section there results:

$$\ddot{\varphi} + \dot{\varphi} \cos \varphi + \frac{1}{4\zeta^2} \sin \varphi = \frac{D}{4\zeta^2 \omega_n^2} \tag{31}$$

Again let $\varphi = x$ and $\dot{\varphi} = y$; the slope of the trajectories becomes

$$\frac{dy}{dx} = - \cos x + \frac{\left(\frac{D}{\omega_n^2}\right) - \sin x}{4\zeta^2 y} \tag{32}$$

The singular points at which the slope becomes indeterminate are now:

$$\left.\begin{aligned} &y = 0, \quad x = \sin^{-1}\left(\frac{D}{\omega_n^2}\right) \pm 2n\pi \\ &\text{and} \\ &y = 0, \quad x = \pi - \sin^{-1}\left(\frac{D}{\omega_n^2}\right) \pm 2n\pi \end{aligned}\right\} (n = 0, 1, 2, \ldots) \tag{33}$$

It is interesting to note that if D, the slope of the excitation, equals the square of the natural frequency of the loop, the two sets of singularities come together; and if

$$D > \omega_n^2 \tag{34}$$

no singular points exist.

It will be shown that inequality (34) is the condition for instability. That is, if the doppler or modulation slope ever satisfies this condition not only can the loop never achieve lock, but even if it was initially in lock it will immediately fall out of lock when the excitation is applied.

The phase-plane plot can be obtained by analog methods using the computer configuration of Fig. 3 with the addition of a constant bias D/ω_n^2 on the first integrator. Figures 9 through 13 were obtained by thus mechanizing Eq. (31) for a damping factor $\zeta = 0.707$ and various levels of the ratio D/ω_n^2.

The following comments may be made concerning these graphs:

1. The singular points are of the same nature with the linear excitation as without it. The only difference is that the stable point is displaced to the right by $\sin^{-1}\left(D/\omega_n^2\right)$ while the saddle point has moved to the left by this amount, as was predicted. Since the stable point represents phase-lock, it is seen that the steady phase-error of a second-order loop with linear excitation is

$$E_{ss} = \sin^{-1}\left(\frac{D}{\omega_n^2}\right)$$

   The linear approximation discussed in Sec. II predicts a steady-state error of D/ω_n^2 which is valid only for small values of the ratio.

2. The trajectories are decidedly asymmetric about the x axis. For low values of D/ω_n^2 (Fig. 9), in the upper

half plane all trajectories above the line B-B are divergent, slowly at first and more noticeably as the error frequency increases. On the other hand, all trajectories below B-B converge toward a stable point either in the same strip or some other strip to the right or left depending on whether the trajectory is in the upper or lower half plane. The line B-B exhibits a periodic behavior (neither locking in nor diverging) which is, however, unstable since the slightest disturbance will tend to push the system either into lock or into complete instability.

Figure 9 verifies the intuitive observation that in order to acquire a positive doppler-shifted frequency it is best to make the VCO frequency lead the input reference (this corresponds to a negative frequency error) and let the increasing doppler shift decrease the error until lock is achieved.

3. As the ratio D/ω_n^2 is increased the line B-B which establishes the limit between stability and instability in the upper half plane descends until at $D/\omega_n^2 = 1/2$ (Fig. 10) it practically coincides with the saddle point asymptotes A-A. Thus, when the ratio reaches this value all trajectories in the lower half plane are drawn into lock, while in the upper half plane lock can never be achieved, unless achieved within the original strip of width 2π.

4. For yet larger values of D/ω_n^2 (Fig. 11) another phenomenon becomes apparent. While most trajectories which start in the lower half plane still achieve lock in some strip, there are some that do not. In particular, any trajectory that passes within the corridor whose lines of demarcation are the extensions of the saddle point asymptotes A-A will be whipped past the x axis into the upper half plane. The width of this corridor in the lower half plane is increased as D/ω_n^2 increases (Fig. 12) and many more trajectories become unstable. As the ratio becomes almost one (Fig. 13) the corridor becomes so wide that only trajectories which began in the immediate vicinity of the stable singularity ever achieve lock.

Finally, when $D/\omega_n^2 \geq 1$ the singularities disappear and no stable point exists. Thus a loop which was originally in lock before the excitation was applied will immediately lose lock. The conclusion which may be drawn from these results is that a second-order loop can acquire a noise-free doppler-shifted or modulated signal with certainty only if the ratio of frequency slope to the square of the natural frequency is less than 1/2, and it can track the signal once lock is achieved only until the ratio becomes unity.

It is of interest to derive an approximate expression for the periodic limiting behavior between stable and divergent trajectories for small D/ω_n^2 (line B-B in Fig. 9). If y is to be periodic $y(\pi) = y(-\pi)$.

Multiplication of Eq. (32) by y and integration between the limits $\pm\pi$ yields:

$$0 = \frac{1}{2}\left[y^2(\pi) - y^2(-\pi)\right] = -\int_{-\pi}^{\pi} y \cos x \, dx + \frac{\pi D}{2\zeta^2 \omega_n^2}$$

Integrating by parts and making use of Eq. (32):

$$0 = \int_{-\pi}^{\pi} \sin x \left(-\cos x + \frac{D}{4\zeta^2 y \omega_n^2} - \frac{\sin x}{4\zeta^2 y}\right) dx + \frac{\pi D}{2\zeta^2 \omega_n^2}$$

For small D and consequently large y_{av} of the periodic behavior this leads to the approximation

$$0 \simeq \frac{-\pi}{4\zeta^2 y_{av}} + \frac{\pi D}{2\zeta^2 \omega_n^2} \qquad (35)$$

or

$$y_{av} \simeq \frac{\omega_n^2}{2D}$$

This can be taken as an approximate expression for pull-in range. In terms of Ω, the condition becomes

$$\Omega < \frac{\zeta \omega_n^3}{D} \qquad (36)$$

For the case of Fig. 9 in which $D/\omega_n^2 = 1/4$, $\zeta = 0.707$, this predicts that $\gamma_{av} \cong 2.0$. It will be noted that this is a fair approximation. The approximation improves as D/ω_n^2 decreases but it is very poor as D/ω_n^2 approaches 1/2.

VI. SECOND-ORDER LOOP WITH IMPERFECT INTEGRATOR

If a passive RC loop filter[2] is used or if the integrator in a second-order loop is not perfect, the loop filter has a transfer function of the form:

$$F(p) = \frac{p + a}{p + \alpha} \tag{37}$$

Substitution of this function into Eq. (3) yields

$$\frac{d\varphi}{dt} + K\left(\frac{p + a}{p + \alpha}\right) \sin\varphi = \dot{\varphi}_s - \omega_c \tag{38}$$

Assuming the input frequency to be constant and letting $\Omega = \dot{\varphi}_s - \omega_c$ this may be written as

$$\frac{d^2\varphi}{dt^2} + \frac{d\varphi}{dt}(\alpha + K)\cos\varphi + aK \sin\varphi = \alpha\Omega \tag{39}$$

To obtain the form of Eq. (9) which represents a second-order loop with perfect integrator, again let $K = 2\zeta\omega_n$, $aK = \omega_n^2$.

---

[2] This was also investigated by Gruen (Ref. 3). Preston and Tellier (Ref. 4) considered the simpler filter $F(p) = \alpha/(p + \alpha)$, which is a sub-class of this case.

Then

$$\frac{d^2\varphi}{dt^2} + \frac{d\varphi}{dt}\left(\alpha + 2\zeta\,\omega_n \cos\varphi\right) + \omega_n^2 \sin\varphi = \alpha\Omega \tag{40}$$

If the time is again normalized, $t = \tau/(2\zeta\,\omega_n)$, and the result is

$$\ddot{\varphi} + \left(\frac{\alpha}{2\zeta\,\omega_n} + \cos\varphi\right)\dot{\varphi} + \frac{1}{4\zeta^2}\sin\varphi = \frac{\alpha\Omega}{4\zeta^2\,\omega_n^2} \tag{41}$$

where

$$\dot{\varphi} = \frac{d\varphi}{d\tau} = \left(\frac{1}{2\zeta\,\omega_n}\right)\frac{d\varphi}{dt}$$

With the convention $\dot{\varphi} = y$, $\varphi = x$

$$\frac{dy}{dx} = -\left(\frac{\alpha}{2\zeta\,\omega_n} + \cos x\right) + \frac{\left(\frac{\alpha\Omega}{\omega_n^2}\right) - \sin x}{4\zeta^2\, y} \tag{42}$$

This indicates that the singularities are at $y = 0$, $x = \sin^{-1}\left(\alpha\Omega/\omega_n^2\right)$ and $x = \pi - \sin^{-1}\left(\alpha\Omega/\omega_n^2\right)$ which implies that for

$$\Omega > \frac{\omega_n^2}{\alpha} \tag{43}$$

there is no stable point and hence the system can not achieve lock. Condition (43) is the upper bound for phase lock; that is, if the input frequency is more than ω_n^2/α radians away from the VCO center, frequency lock-on is impossible on the basis of the singular point behavior.

However, for lesser Ω pull-in may not occur even though a stable point exists in the phase-plane. Examination of Figs. 14-18,

the analog computer solutions of Eq. 41, bears this out. In all cases $\zeta = 0.707$ and $\alpha/2\zeta\,\omega_n = 0.1$. The behavior varies with the value of Ω. Condition (43) requires $\alpha\Omega/\omega_n^2 < 1$ for lock to occur. In Fig. 14 $\alpha\Omega/\omega_n^2 = 0.4$ and pull-in is quite apparent. It should be noted that given $\alpha/2\zeta\,\omega_n = 0.1$ and $\zeta = 0.707 = 1/\sqrt{2}$ then $\Omega/\omega_n = 2\sqrt{2}$. Thus, if the VCO was initially at its center frequency, then the initial value of $y = \dot{\phi} = \Omega/2\zeta\,\omega_n = 2$. On the other hand, if initially the VCO was not at its center frequency because it had been tracking a signal of another frequency, then the initial value of y is not restricted. It seems apparent from Fig. 14 that pull-in occurs for all initial values of y when $\Omega/\omega_n = 2\sqrt{2}$.

Figure 16 represents the solution for $\alpha\Omega/\omega_n^2 = 0.7$ or $\Omega/\omega_n = 7\sqrt{2}/2$. A limit cycle exists about $y_{av} = 2.5$ toward which all higher trajectories converge. If the VCO is at ω_c initially then initially $y = \Omega/2\zeta\,\omega_n = 3.5$ and the system converges to the limit cycle and exhibits a periodically varying frequency error as long as the input frequency remains constant. If the initial frequency of the VCO is not ω_c, one of three situations may exist (see Fig. 19).

1. The initial VCO frequency (ω_0) lies further from the signal frequency (ω_s) than does the VCO center frequency (ω_c). Then the initial value of $y > \Omega/2\zeta\,\omega_n$ and the trajectory will converge to the limit cycle.
2. ω_0 lies nearer to ω_s than does ω_c; then initially $0 < y < \Omega/2\zeta\,\omega_n$ and the system will lock in if y is sufficiently small, or otherwise converge to the limit cycle. Figure 16, in fact, shows this behavior in form

of an unstable limit cycle below the aforementioned stable one. If y initially lies below this unstable limit cycle, lock-in occurs. If it lies between the limit cycles it will converge to the higher one.

(3) ω_0 lies on the other side of ω_s from ω_c; then initially y is negative and the system seems to lock in always.

Figure 15 ($\alpha\Omega/\omega_n^2 = 0.6$ and $\Omega/\omega_n = 3\sqrt{2}$) represents a behavior intermediate to those already considered. Pull-in occurs throughout but the rate is slower near the region in which a limit cycle occurs for the case of Fig. 16. Thus, it appears that if the VCO is initially at ω_c, for $\zeta = 0.707$ and $\alpha/2\zeta\,\omega_n = 0.1$ the limit for pull-in lies in the region

$$3\sqrt{2} < \frac{\Omega}{\omega_n} < \frac{7}{2}\sqrt{2} \tag{44}$$

Figures 17 and 18 represent the solution for $\Omega/\omega_n = 4\sqrt{2}$ and $9/2\sqrt{2}$. If the VCO is initially at ω_c, the initial values of y are at 4 and 4.5 respectively and pull-in does not occur, of course. The stable limit cycle is again in evidence and furthermore, if y is initially negative (case 3 above), lock-in is not assured since those trajectories which pass through a strip determined by the asymptotes of the saddle point will converge to the limit cycle.

An approximate analytical derivation of the pull-in range follows. Returning to Eq. (40), letting the frequency error $d\varphi/dt = \omega$ and dividing by ω yields:

$$\frac{d\omega}{d\varphi} = -(\alpha + 2\zeta\,\omega_n \cos\varphi) + \frac{\alpha\Omega - \omega_n^2 \sin\varphi}{\omega} \tag{45}$$

Multiplication by ω followed by integration from $\varphi = -\pi$ to $+\pi$ yields measure of the decay or rise in frequency error during one cycle.

$$\frac{1}{2}\left[\omega^2(\pi) - \omega^2(-\pi)\right] = 2\pi\alpha\Omega - \int_{-\pi}^{\pi} \omega(\alpha + 2\zeta\,\omega_n \cos\varphi)\, d\varphi \qquad (46)$$

Integrating by parts using Eq. (45)

$$\frac{1}{2}\left[\omega^2(\pi) - \omega^2(-\pi)\right] = 2\pi\alpha\Omega - \pi\alpha\left[\omega(\pi) + \omega(-\pi)\right] + \int_{\pi}^{\pi} (\alpha\varphi + 2\zeta\,\omega_n \sin\varphi)\left(-\alpha - 2\zeta\,\omega_n \cos\varphi + \frac{\alpha\Omega}{\omega} - \frac{\omega_n^2 \sin\varphi}{\omega}\right) d\varphi \qquad (47)$$

Making the assumption that the frequency error ω is large compared to ω_n, the terms in ω in the integrand will not change appreciably during one cycle, so that throughout the cycle $\omega \simeq \omega(-\pi)$ for $-\pi < \varphi < \pi$ Then:

$$\frac{1}{2}\left[\omega^2(\pi) - \omega^2(-\pi)\right] \simeq 2\pi\left\{\alpha\Omega - \alpha\left[\omega(-\pi)\right] - \frac{\omega_n^2(\alpha + \zeta\omega_n)}{\omega(-\pi)}\right\}$$
$$= -\frac{2\pi\alpha}{\omega(-\pi)}\left\{\left[\omega(-\pi)\right]^2 - \Omega\left[\omega(-\pi)\right] + \omega_n^2\left(\frac{\zeta\,\omega_n}{\alpha} + 1\right)\right\} \qquad (48)$$

The trajectories will always decay when the right hand side of this equation is negative, which occurs for the following range of Ω:[3]

[3] Gruen's result for pull-in range was obtained by an empirical technique for $\omega_n/\alpha >> 1$. It is more pessimistic than condition (49) by a factor of $\sqrt{2}$.

$$\Omega < 2\,\omega_n \sqrt{\frac{\zeta\,\omega_n}{\alpha} + 1} \tag{49}$$

For the cases investigated $\alpha/2\zeta\,\omega_n = 0.1$ so that the approximate condition for pull-in when the VCO is initially at its center frequency will be

$$\frac{\Omega}{\omega_n} < 2\sqrt{6} = (3.46)\sqrt{2}$$

This lies in the region determined on the analog computer (Eq. 44).

VII. THIRD-ORDER LOOP TRACKING BEHAVIOR

Section V has demonstrated the limitations of the second-order loop in tracking frequency-variable signals. It is of interest to investigate the possibility of extending some of these limitations by inserting a second integrator in the loop filter. It develops that pull-in behavior is less stable for a third-order loop than for one of second order but it will be shown that the tracking range for a loop initially in lock can be extended by means of the second integrator. The loop filter transfer function is

$$F(p) = 1 + \frac{a}{p} + \frac{b}{p^2} \tag{50}$$

and Eq. (3) becomes

$$p\varphi + \frac{Kp^2 + aKp + bK}{p^2}(\sin\varphi) = \Omega + Dt \tag{51}$$

Letting $K = 2\zeta\,\omega_n$; $aK = \omega_n^2$ and differentiating

$$p^2\varphi + \left(2\zeta\,\omega_n\,p + \omega_n^2 + \frac{2\zeta\,\omega_n}{p}\,b\right)(\sin\varphi) = D \tag{52}$$

Making the substitution

$$t = \frac{\tau}{2\zeta\,\omega_n} \text{ and dropping the operational notation}$$

$$4\zeta^2\,\omega_n^2\left(\frac{d^2\varphi}{d\tau^2}\right) + 4\zeta^2\,\omega_n^2\cos\varphi\left(\frac{d\varphi}{d\tau}\right) + \omega_n^2\sin\varphi \tag{53}$$

$$+ b\int \sin\varphi\,d\tau = D$$

Normalizing and letting $\frac{d\varphi}{d\tau} = \dot{\varphi}$

$$\ddot{\varphi} + \dot{\varphi}\cos\varphi + \frac{1}{4\zeta^2}\sin\varphi + \frac{b}{4\zeta^2\,\omega_n^2}\int \sin\varphi\,d\tau = \frac{D}{4\zeta^2\,\omega_n^2} \tag{54}$$

Conventional phase-plane techniques are not applicable to third-order differential equations because there are three initial conditions corresponding to each of the three dynamic variables to be considered: phase, frequency, and frequency rate (or displacement, velocity, and acceleration in mechanical systems). In principle, the trajectories of a third-order equation could be described in three dimensions. However, an attempt to project these trajectories for a multitude of initial conditions on a plane will generate such a confused diagram that little of a general nature can be deduced.

On the other hand, if one limits oneself to a single set of initial conditions, a meaningful projection of the trajectory onto the φ - $\dot{\varphi}$ plane will result. The set of initial conditions of greatest interest is $\varphi = d\varphi/dt = 0$; $d^2\varphi/dt^2 = D$; that is, the loop is initially in lock so that the frequency and phase errors are zero when the reference frequency begins to change linearly.

The analog computer program of Fig. 3 can easily be modified to include another integrator. Figure 20 represents a series of trajectories projected on the φ - $\dot{\varphi}$ plane. In all cases $\zeta = 0.707$ and $D/\omega_n^2 = 1/2$. In the hypothetical three dimensional "phase space" the trajectories initiate at $\ddot{\varphi} = D/4\zeta^2\,\omega_n^2$ and terminate on the φ axis ($\dot{\varphi} = \ddot{\varphi} = 0$). Figure 20 (a) shows the behavior of a second-order loop ($b = 0$) with these initial conditions. The terminal or steady-state phase is $\sin^{-1}(D/\omega_n^2)$ as was pointed out in Sec. V. Addition of the second integrator causes the steady-state phase to become zero with increasing rapidity as b/ω_n^2 increases. The peak phase error also diminishes for increasing values of b/ω_n^2 at the cost, however, of decreased system damping which results in increased rms phase error (Figs. 20 (b) - 20 (f)). Finally, as b/ω_n^2 approaches unity the loop becomes unstable.

The advantages secured by increasing the order of the loop are more evident in Fig. 21. Here $\zeta = .707$ again but $D/\omega_n^2 = 1$. It was shown in Sec. V that for this and higher values of linear frequency shift the loop was incapable of tracking. Figure 21(a) ($b/\omega_n^2 = 0$) substantiates this fact. On the other hand, even the smallest magnitude of the second integrator produces zero steady-state

phase error. The peak-phase error is decreased by increasing b/ω_n^2 but as b/ω_n^2 approaches unity the rms error increases until near $b/\omega_n^2 = 1$ the system is again unstable.

Similar behavior is apparent in Figs. 22, 23, and 24 except that as D/ω_n^2 increases an increasingly greater value of b/ω_n^2 is required to keep the loop in lock. Finally, when D/ω_n^2 is near 2 a value of b/ω_n^2 near unity is required. However, it is evident from Figs. 20(g) to 24 (f) that for this value of b/ω_n^2 the system is unstable. The range of values that b/ω_n^2 may take on in order for the loop to remain in lock is plotted as a function of D/ω_n^2 in Fig. 25 - 27 for $\zeta = 0.707$, 0.5, and 1 respectively. The cross-hatched area represents permissible values of b/ω_n^2. Clearly, for linear frequency shifts the third-order loop has extended the tracking range to approximately twice that of the second-order loop for a damping factor, ζ, of the latter equal to 0.707 and even further for higher values of ζ.

A theoretical explanation of the oscillatory behavior for b/ω_n^2 near or above unity is possible. The characteristic polynomial of the loop (Eq. 52) can be rewritten as

$$\left[p^3 + (2\zeta\, \omega_n p^2 + \omega_n^2 p + 2\zeta\, \omega_n b)\, \frac{\sin \varphi}{\varphi} \right] \varphi = 0 \qquad (55)$$

The Routh-Hurwitz test on the polynomial yields the fact that for

$$\frac{b}{\omega_n^2} \geq \frac{\sin \varphi}{\varphi} \qquad (56)$$

the loop is unstable. This indicates that if in a particular trajectory the phase error reaches such a value that condition (56) is

satisfied the trajectory will become unstable. Clearly, if $b/\omega_n^2 = 1$ the condition is satisfied for all φ and the system is always unstable. This fact is also borne out by the linear model which follows from the approximation $\sin \varphi \simeq \varphi$. Application of the Routh-Hurwitz test to the linear equation sets the instability criterion as $b/\omega_n^2 \geq 1$.

The tracking behavior of the third-order loop does not seem to be much different than that of the second-order loop for $D/\omega_n^2 < 1$. For $D/\omega_n^2 > 1$, the region for which the second-order loop can not lock in, there is a limited range of D/ω_n^2 for which the proper choice of b/ω_n^2 will secure lock. The pull-in behavior when the VCO is not initially tracking the reference signal seems to be less stable than for a second-order loop. However, generalizations can not be made because of the complexity of the phase-space trajectories.

VIII. NOISE AND LOOP NOISE-BANDWIDTH

Some comments are in order on the effect of noise on the pull-in and tracking behavior. A small amount of phase and frequency jitter due to noise will not affect the phase-plane trajectories significantly; it will result only in hash being superimposed on the trajectories. However, the bias due to the signal frequency error is still the dominating factor which causes the loop to pull in and a small jitter on the trajectories will not affect the number of cycles required to achieve lock. On the other hand, if the input noise is significant, particularly when the initial frequency error is large, the disturbance on the trajectory may be such that a different number of cycles will be required for the system to achieve lock.

When the loop is in lock and tracking a noisy signal it is convenient to consider the linear model which results from the approximation $\sin \varphi \simeq \varphi$. This enables one to analyze the propagation of noise through the system and even to derive the form of the loop filter which will result in a Wiener optimum linear system (see Ref. 1). A key parameter which results from the consideration of noise in the system is the loop noise-bandwidth B_L defined as

$$2B_L = \frac{1}{2\pi j} \int_{-j\infty}^{j\infty} \left| H(p) \right|^2 dp \qquad (57)$$

where $H(p)$ is the transfer function of the linearized loop from input phase to the output phase of the VCO. The basis of this definition lies in the fact that a flat noise spectral density of magnitude Φ at the input of the linear system will produce at the output a noise power $2\Phi B_L$. Thus B_L is the bandwidth of the ideal square-cutoff low-pass filter which produces the same amount of noise power at its output as does the linear system whose realizable transfer function is $H(p)$.

With this definition, the loop noise-bandwidths of the various filters may be considered. For the first-order loop the linearized transfer function follows from Eqs. (3) and (4).

$$H(p) = \frac{\varphi_0(p)}{\varphi_s(p)} = \frac{K}{p + K} \qquad (58)$$

where $\varphi_0 = \varphi_s - \varphi$ is the output phase of the VCO and $F(p) = 1$. Applying the definition (57) results in a loop noise-bandwidth for

the first-order loop of

$$B_L = \frac{K}{4} \tag{59}$$

Then the transfer function (58) can be expressed in terms of B_L:

$$H(p) = \frac{4\,B_L}{p + 4\,B_L} \tag{60}$$

Rechtin has shown (Ref. 1) that to minimize the output noise power and simultaneously to maintain the rms phase error due to a step change in frequency within a given bound, the optimum linear filter will be of second order and of the form

$$H(p) = \frac{\omega_n^2 + \sqrt{2}\,\omega_n p}{\omega_n^2 + \sqrt{2}\,\omega_n p + p^2} \tag{61}$$

From the denominator which is the characteristic polynomial it is clear that the damping factor of this optimum loop is $\zeta = 1/\sqrt{2} = .707$. Application of Eq. (57) yields a

$$B_L = \frac{3\omega_n}{4\sqrt{2}} \tag{62}$$

Then

$$H(p) = \frac{1 + \frac{3}{4\,B_L}\,p}{1 + \frac{3}{4\,B_L}\,p + \frac{9}{32\,B_L^2}\,p^2} \tag{63}$$

Also it is shown that to minimize the output noise power and simultaneously to maintain the rms phase error due to a linearly varying frequency input within a given bound, the optimum filter will be of third order and its transfer function in terms of the loop noise bandwidth is

$$H(p) = \frac{1 + \frac{5}{3 B_L} p + \frac{25}{18 B_L^2} p^2}{1 + \frac{5}{3 B_L} p + \frac{25}{18 B_L^2} p^2 + \frac{125}{216 B_L^3} p^3} \tag{64}$$

The characteristic polynomial of the system is then

$$p^3 + \frac{12}{5} B_L p^2 + \frac{72}{25} B_L^2 p + \frac{216}{125} B_L^3$$

Comparison of this with that of Eq. (55) for which the linearizing assumption is made results in the following values for the ζ, ω_n, and b parameters in terms of B_L.

$$\omega_n = \frac{6\sqrt{2}}{5} B_L$$

$$\zeta = \frac{1}{\sqrt{2}} = .707$$

$$b = \frac{18}{25} B_L^2$$

Also

$$\frac{b}{\omega_n^2} = \frac{1}{4} \tag{65}$$

IX. SUMMARY OF RESULTS

The various conclusions relative to the filters and signals considered are summarized in terms of both the notations which have been introduced

1. First-Order Loop (Sec. III.)
   a. Pull-in range

$$\Omega < K \frac{\text{rad}}{\text{sec}} \text{ or } \Omega < 4 B_L \frac{\text{rad}}{\text{sec}}$$

   b. Pull-in time for initial frequency error, Ω

$$t = \int_{\varphi_{initial}}^{\varphi_{final}} \frac{d\varphi}{\Omega - K \sin \varphi} = \int_{\varphi_{initial}}^{\varphi_{final}} \frac{d\varphi}{\Omega - 4 B_L \sin \varphi}$$

The integral is evaluated in the standard tables.

2. Second-Order Loop (Perfect Integrator); Constant Reference Frequency (Sec. IV.)
   a. Pull-in range is infinite
   b. Pull-in time for large initial frequency error, Ω

$$t \approx \frac{\Omega^2}{2\zeta\ \omega_n{}^3} \text{ sec}$$

A more accurate expression for smaller Ω is given by Eq. (28)

For optimum loop (using Eq. 62)

$$t \approx \frac{27\ \Omega^2}{256\ B_L{}^3} \text{ sec}$$

3. Second-Order Loop (Perfect Integrator); Linearly Varying Reference Frequency or Constant VCO Drift at Rate D rad/sec^2 (Sec. V)

   a. Approximate pull-in range for $D/\omega_n{}^2 < 1/2$

$$\Omega < \frac{\zeta\omega_n{}^3}{D} \frac{\text{rad}}{\text{sec}}$$

for optimum loop when $D/B_L{}^2 < 16/9$

$$\Omega < \frac{128 B_L{}^3}{27\ D} \frac{\text{rad}}{\text{sec}}$$

   b. Maximum rate which can be tracked

$$D = \omega_n{}^2 \frac{\text{rad}}{\text{sec}^2}$$

for optimum loop

$$D = \frac{32}{9} B_L{}^2 \frac{\text{rad}}{\text{sec}^2}$$

4. Second-Order Loop (Imperfect Integrator) Constant Reference Frequency (Sec. VI)

Pull-in range

$$\Omega < 2\,\omega_n \sqrt{\frac{\zeta\,\omega_n}{\alpha} + 1}\ \frac{\text{rad}}{\text{sec}}$$

where α is inverse time constant of filter.

For optimum loop

$$\Omega < \frac{8\sqrt{2}\,B_L}{3}\ \sqrt{\frac{4\,B_L}{3\alpha} + 1}\ \frac{\text{rad}}{\text{sec}}$$

5. Third-Order Loop (Sec. VII)

Tracking range can be extended beyond $D/\omega_n^2 = 1$ by means of a second integrator in the loop filter. Figure 25 indicates that if in a second order loop, whose damping factor $\zeta = 0.707$, a second integrator is introduced, the tracking range can be extended to $D/\omega_n^2 = 1.83$ by making the normalized value of the second integrator constant $b/\omega_n^2 = 0.65$.

The optimum third order loop in terms of the other set of parameters has $\zeta = 0.707$, $\omega_n = 6\sqrt{2/5}\,B_L$ and $b/\omega_n^2 = 1/4$. Its tracking range extends to

$$\frac{D}{\omega_n^2} = 1.5 \text{ or } \frac{D}{B_L^2} = \frac{75}{144}$$

The reason that b/ω_n^2 is chosen in this case to yield a non-maximum tracking range is that the optimum loop must strike a compromise between tracking accuracy and output noise power, so that optimizing a composite of the two is preferrable to optimizing either one.

Unclassified NOMENCLATURE
Classified - Title or first line of text

A - A = saddle point asymptotes

a = first-order integrator gain

B - B = periodic limit of lock-in

B_L = loop noise-bandwidth

b = second-order integrator gain

C_1 = reference signal amplitude

C_2 = VCO output amplitude

D = linear rate of frequency variation

E_{SS} = steady-state phase error

e_d = multiplier output

F(p) = filter transfer function

H(p) = loop transfer function

$K_0 = C_1C_2$

K_1 = filter DC gain

K_2 = VCO gain

K = loop gain

p = Laplace operator

t = time variable

X = φ phase error

y = $\dot{\varphi}$ frequency error

y_A = value of y along A - A

y_0 = initial y

y_{av} = average value of periodic trajectory

α = inverse time constant of filter with imperfect integrator

β = linear decrease in y per cycle of x

Last line of text or footnote

NOMENCLATURE (Cont'd)

ζ = loop damping factor

τ = normalized time variable

φ = phase error

φ_s = reference signal phase

φ_0 = VCO output phase

$\omega = \dot{\varphi}$ frequency error

$\omega_S = \dot{\varphi}_S$ reference signal frequency

ω_c = VCO center frequency

ω_h = loop natural frequency

ω_0 = initial VCO frequency

$\Omega = \omega_S - \omega_c$

Ω_0 = initial Ω

REFERENCES

1. Jaffe, R. M. and Rechtin, E., "Design and Performance of Phase-Lock Circuits Capable of Near-Optimum Performance Over a Wide Range of Input Signal and Noise Levels," IRE Transactions on Information Theory, IT-1, No. 1: 66-76, March 1955.

2. Gilchriest, C. E., "Application of the Phase-Locked Loop to Telemetry as a Discriminator or Tracking Filter," IRE Transactions on Telemetry and Remote Control, TRC-4, No. 1: 20-35, June 1958.

3. Gruen, W. J., "Theory of A.F.C. Synchronization," Proceedings of IRE, 41, 8:1043-8, August, 1953.

4. Preston, G. W. and Tellier, J. C., "The Lock-in Performance of an A.F.C. Circuit," Proceedings of IRE, 41 2:249-51, February 1953.

5. Richman, D., "Color-Carrier Reference Phase Synchronization in NTSC Color Television," Proceedings of IRE, 106-133, January 1954.

6. Andronow, A. A. and Chaikin, C. E., Theory of Oscillations, Princeton University Press, Princeton, New Jersey, 1949.

7. Truxall, J. G., Automatic Feedback Control System Synthesis, (Chapter 11), McGraw-Hill Book Co., Inc., New York, New York, 1955.

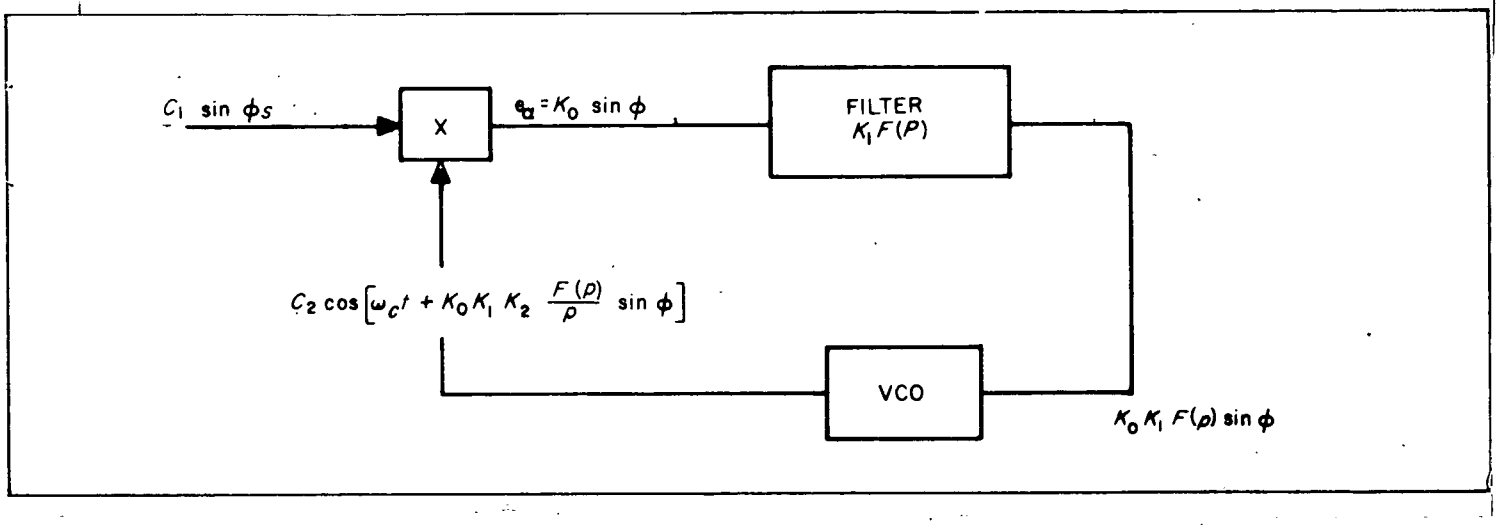

Fig. 1. Phase-Locked Loop

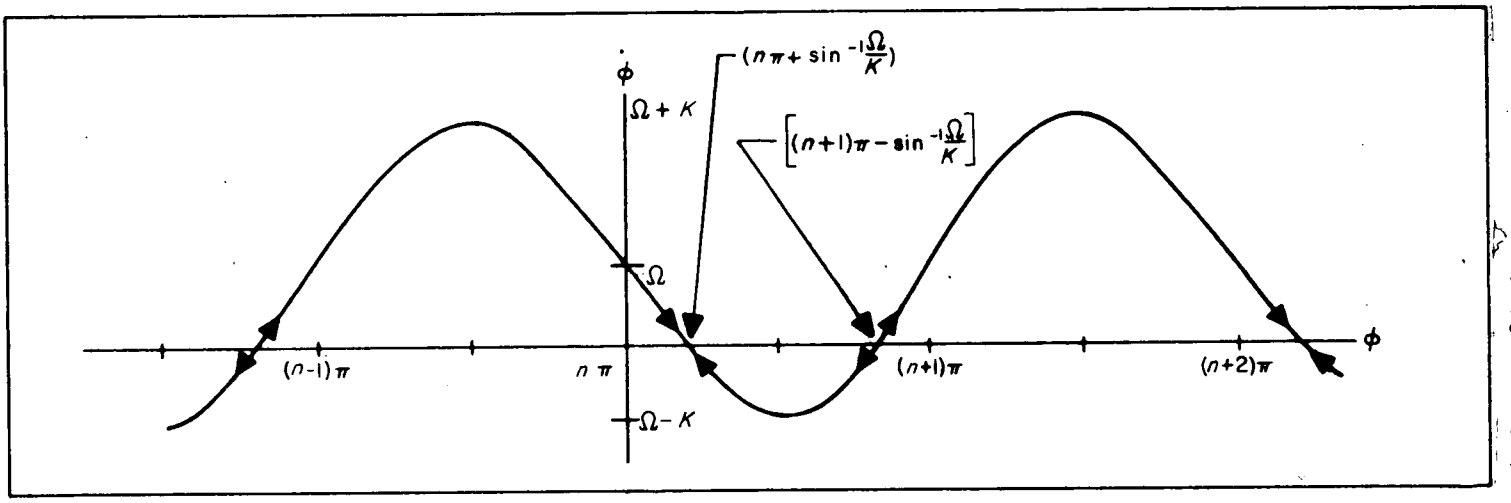

Fig. 2. First-Order Loop Pull-in Behavior (n even integer)

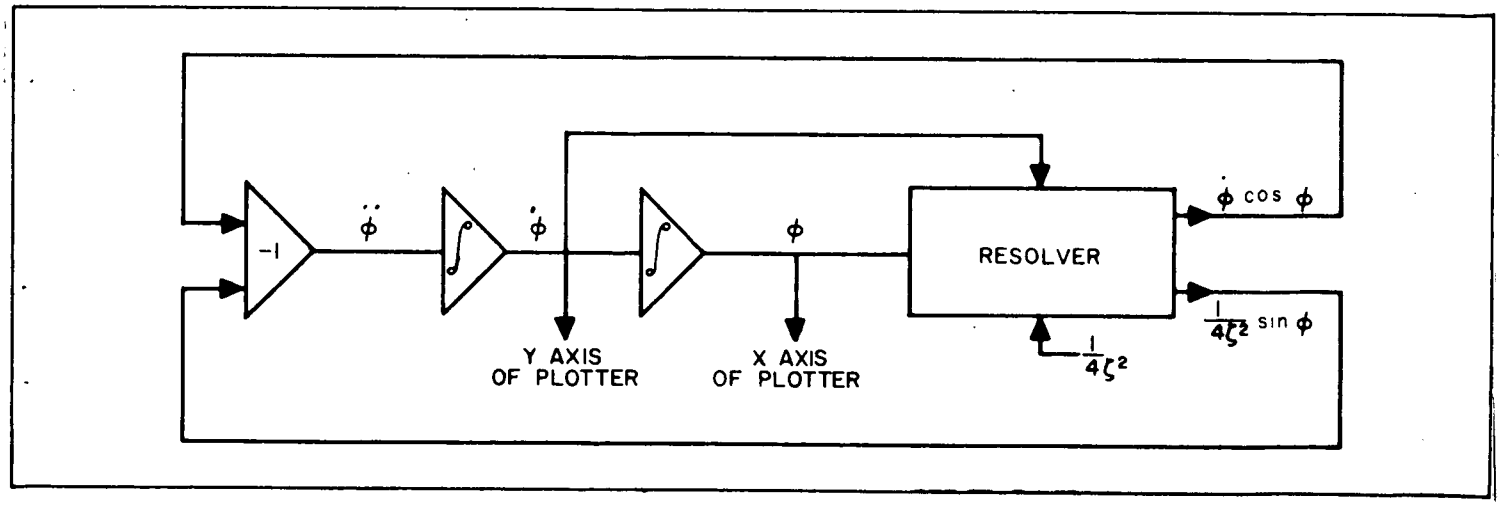

Fig. 3. Basic Analog Computer Mechanization

CLASSIFICATION (if any)

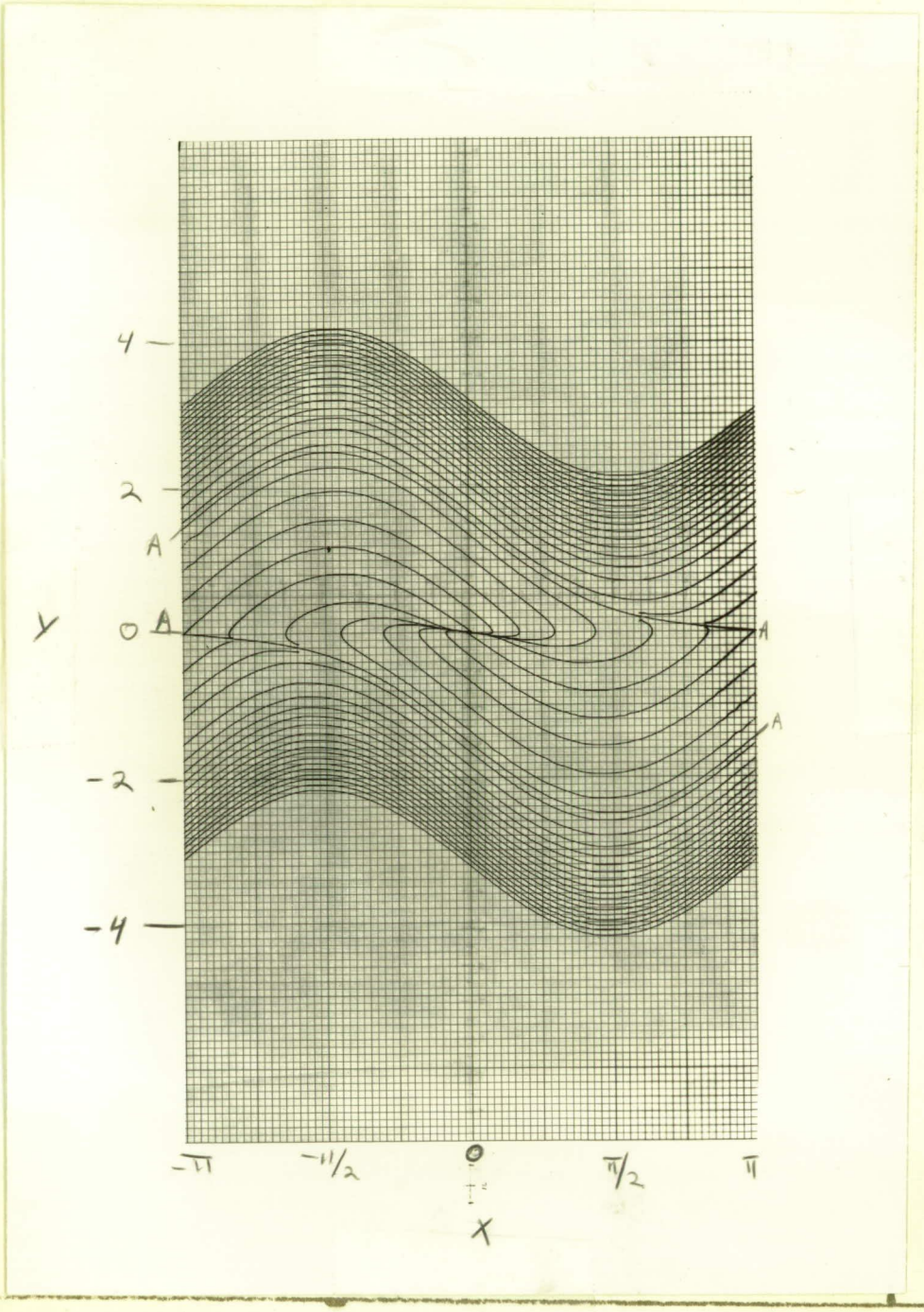

Fig. 4. $\zeta = 1.414$ (overdamped)

t line of text

t line of text

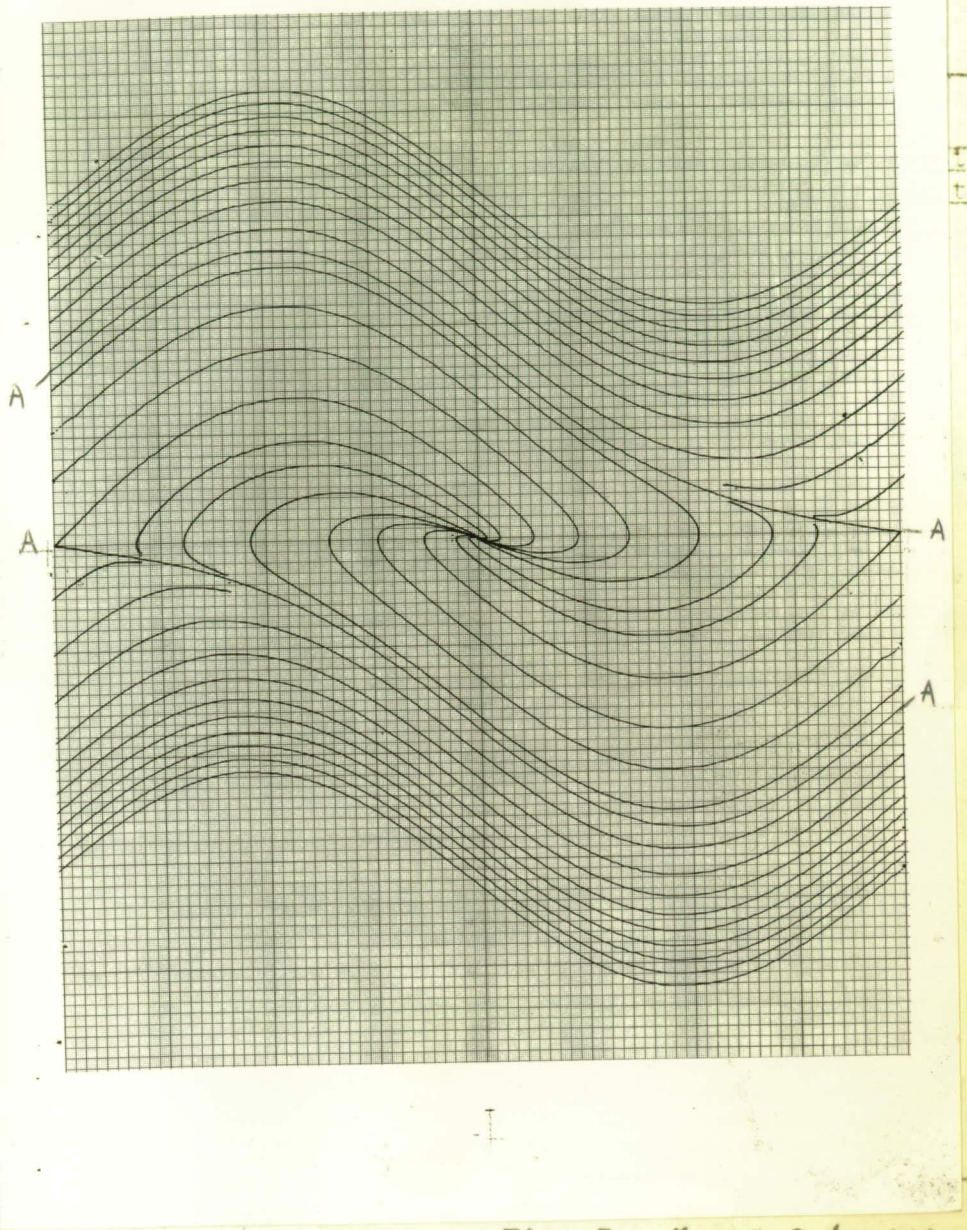

Fig. 5. $\zeta = 1.0$ (critically damped)

Last line of text or footnote

CLASSIFICATION (if any)

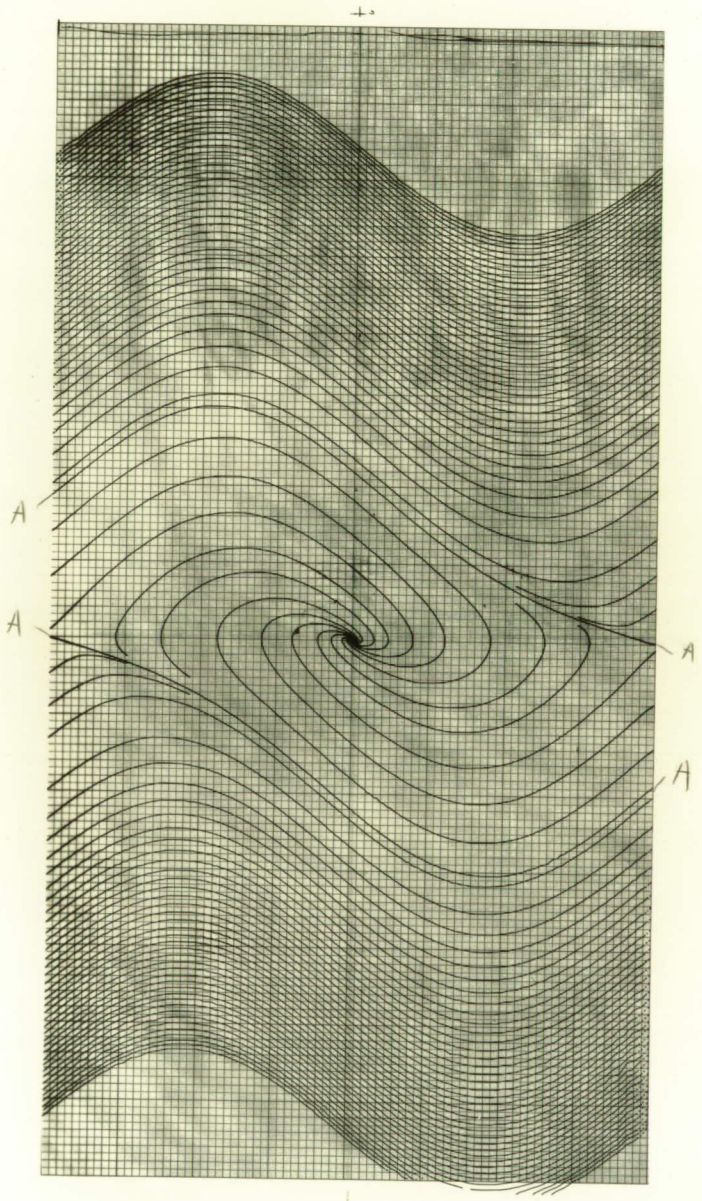

Fig. 6. $\zeta = 0.707$

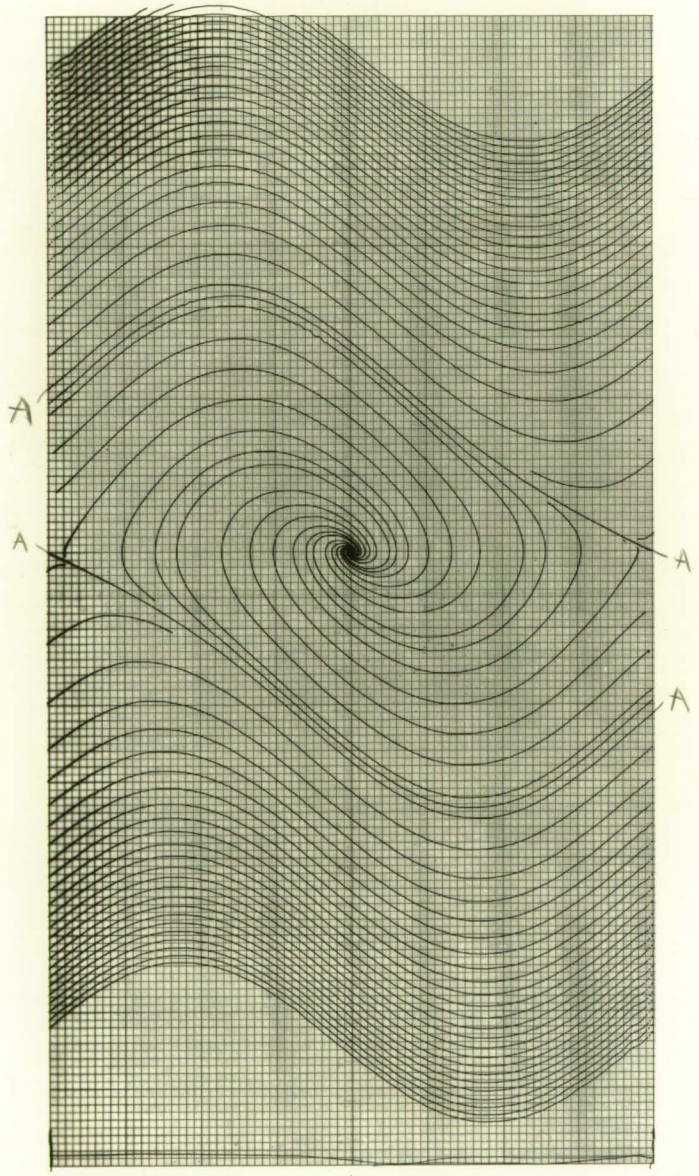

Fig. 7. $\zeta = 0.5$

Fig 8

7 × 5 ↑

Red 78%

Fig. 8. Limit of Frequency-Lock as a Function of Damping

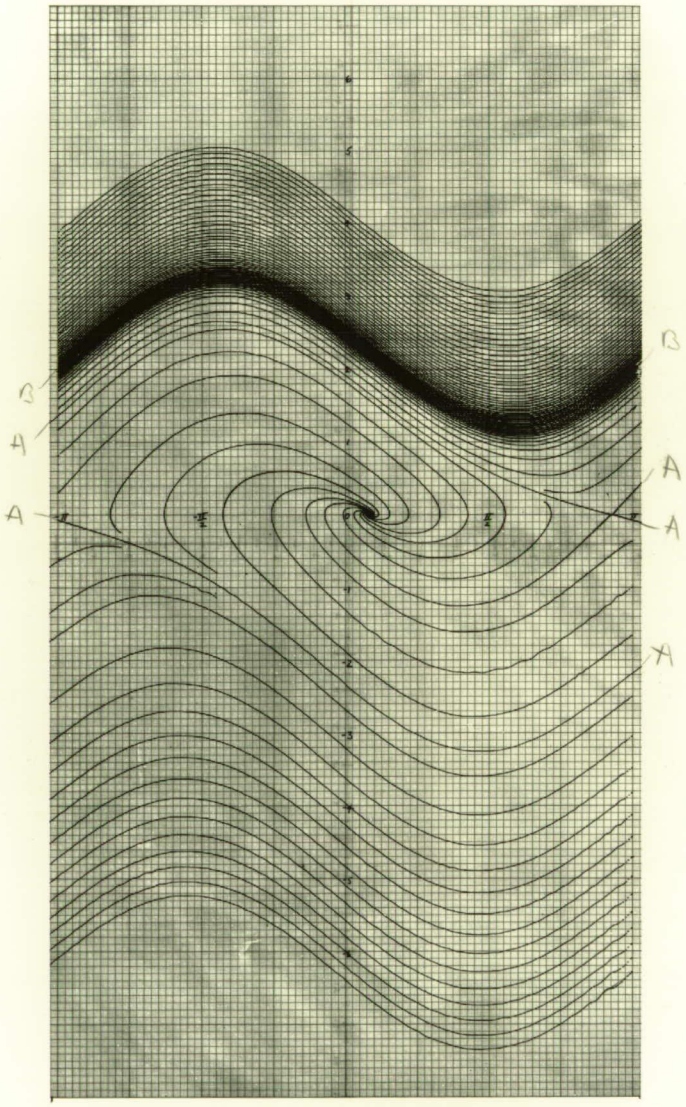

Fig. 9. $\zeta = 0.707$, $D/\omega_n^2 = 1/4$,
$\sin^{-1}(D/\omega_n^2) = 14.5^\circ = 0.08\,\pi$ rad

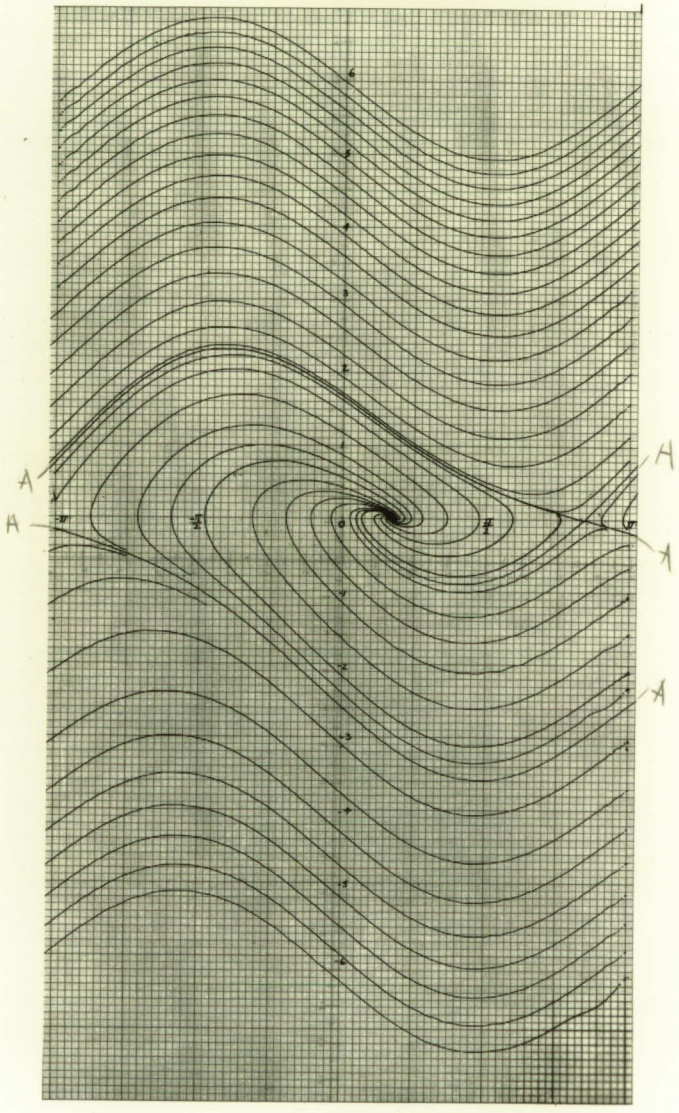

Fig. 10. $\zeta = 0.707$, $D/\omega_n^2 = 1/2$,
$\sin^{-1}(D/\omega_n^2) = 30.0° = \pi/6$ rad

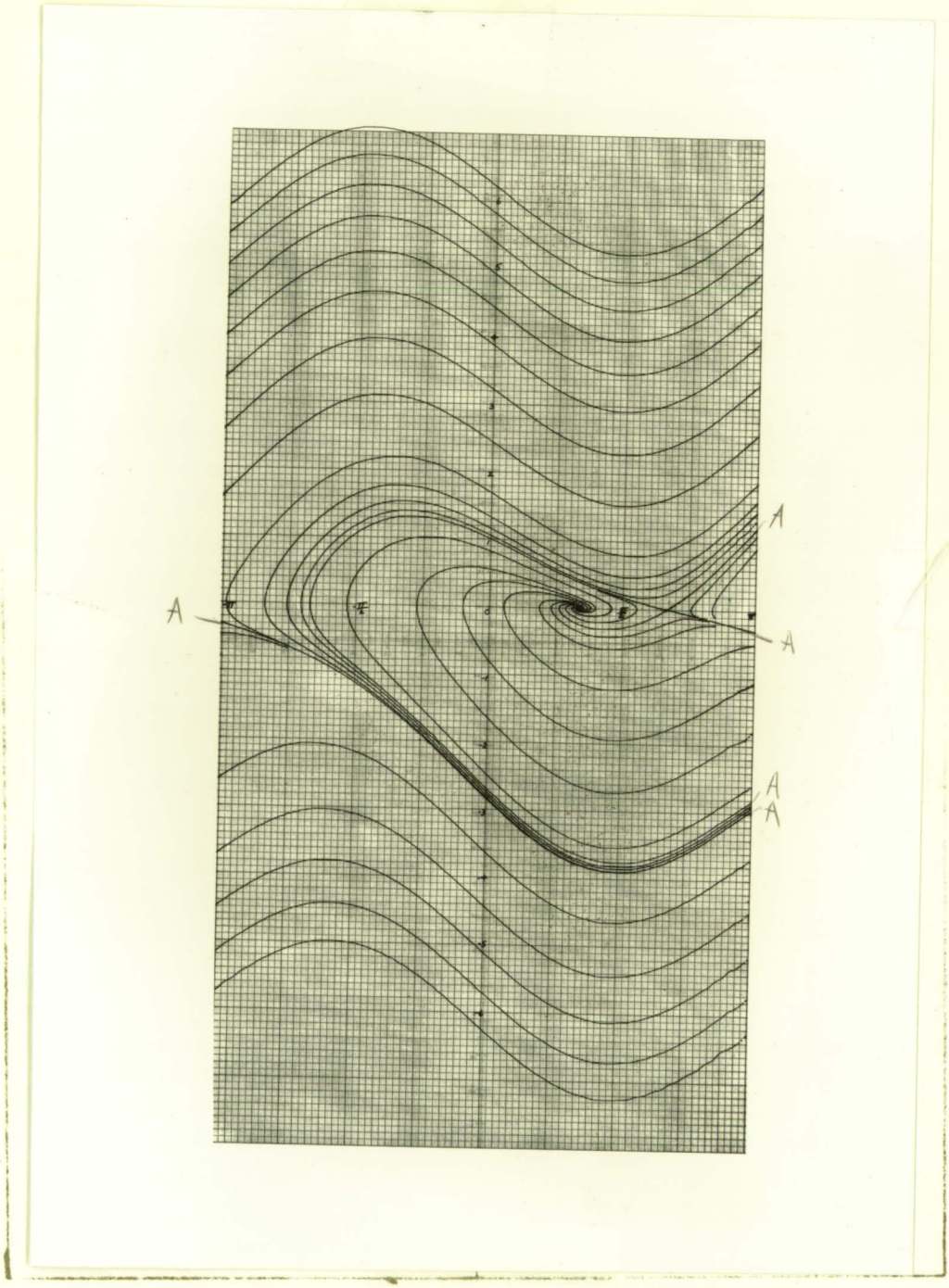

Fig. 11. $\zeta = 0.707$, $D/\omega_n^2 = \sqrt{3}/2 = 0.867$, $\sin^{-1}(D/\omega_n^2) = 60° = \pi/3$ rad

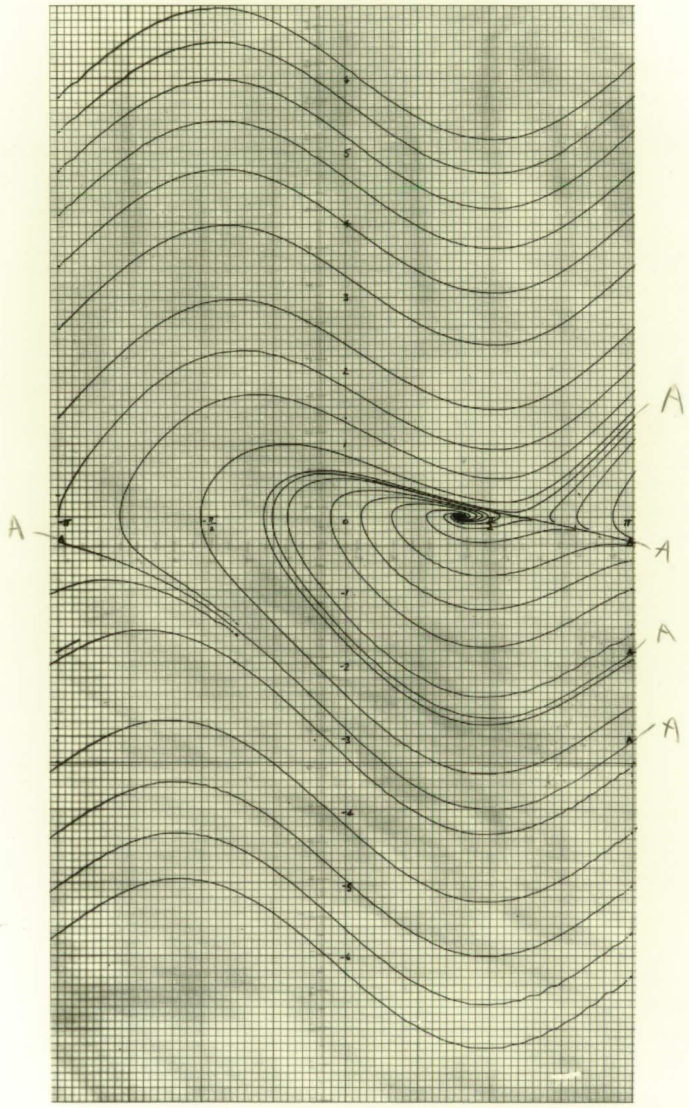

Fig. 12. $\zeta = 0.707$, $D/\omega_n^2 = 0.95$,

$\sin^{-1}(D/\omega_n^2) = 72^\circ = 2/5\ \pi$ rad

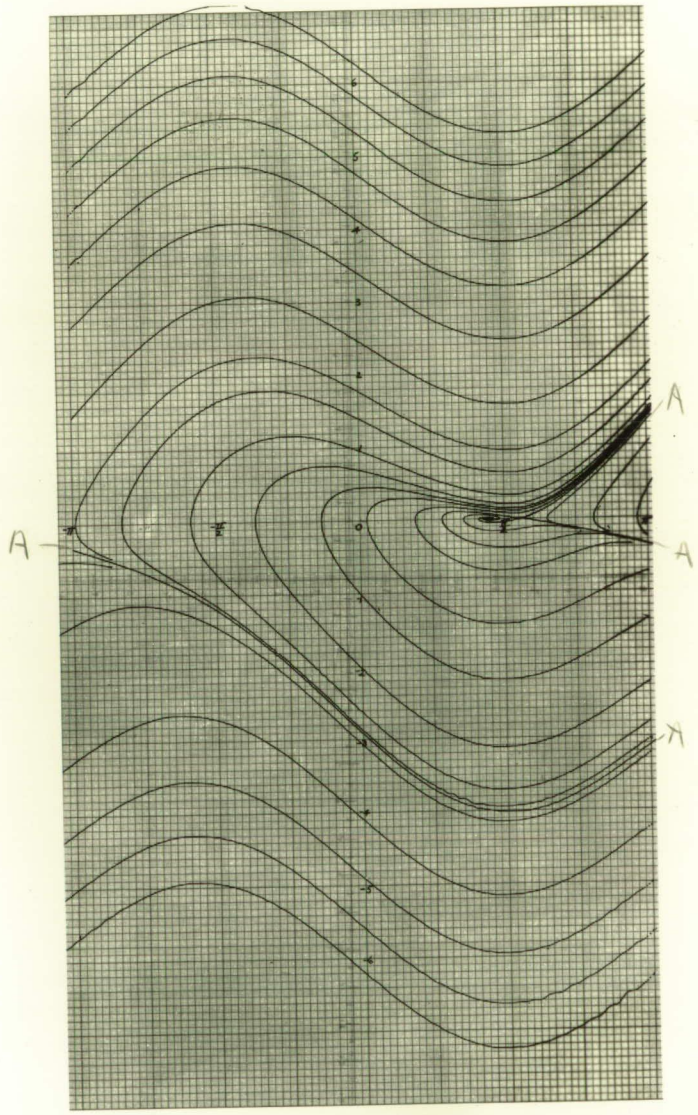

Fig. 13. $\zeta = 0.707$, $D/\omega_n^2 = 0.985$,
$\sin^{-1}(D/\omega_n^2) = 80.0^\circ = 4\pi/9$ rad

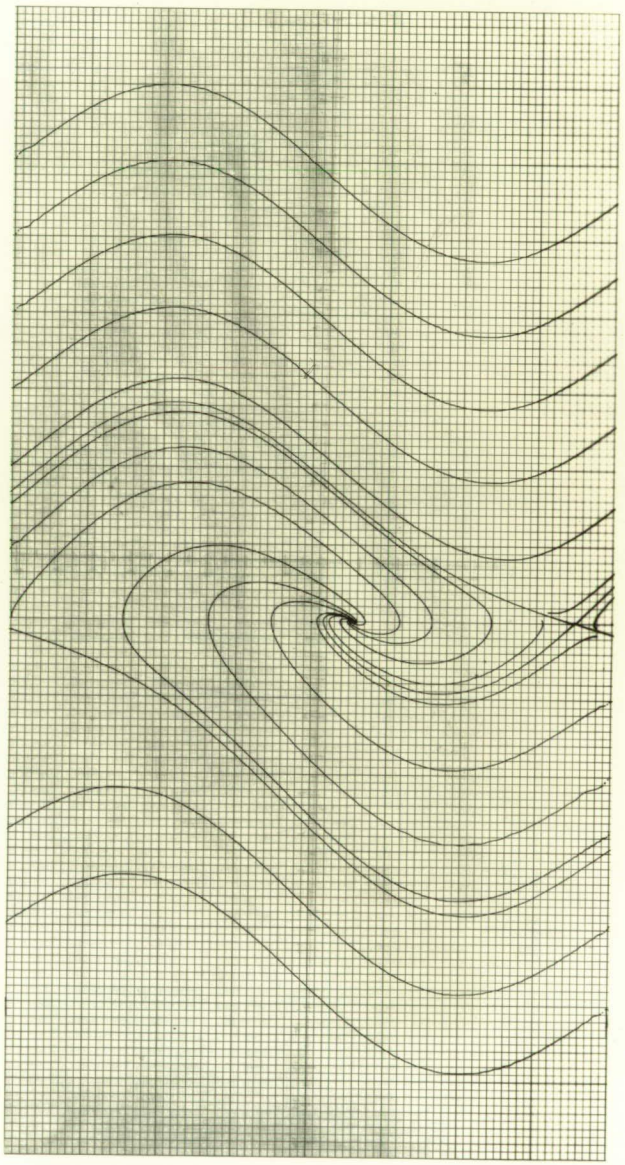

Fig. 14. $\zeta = 0.707$, $a/2\zeta\omega_n = 0.1$,
$a\Omega/\omega_n^2 = 0.4$

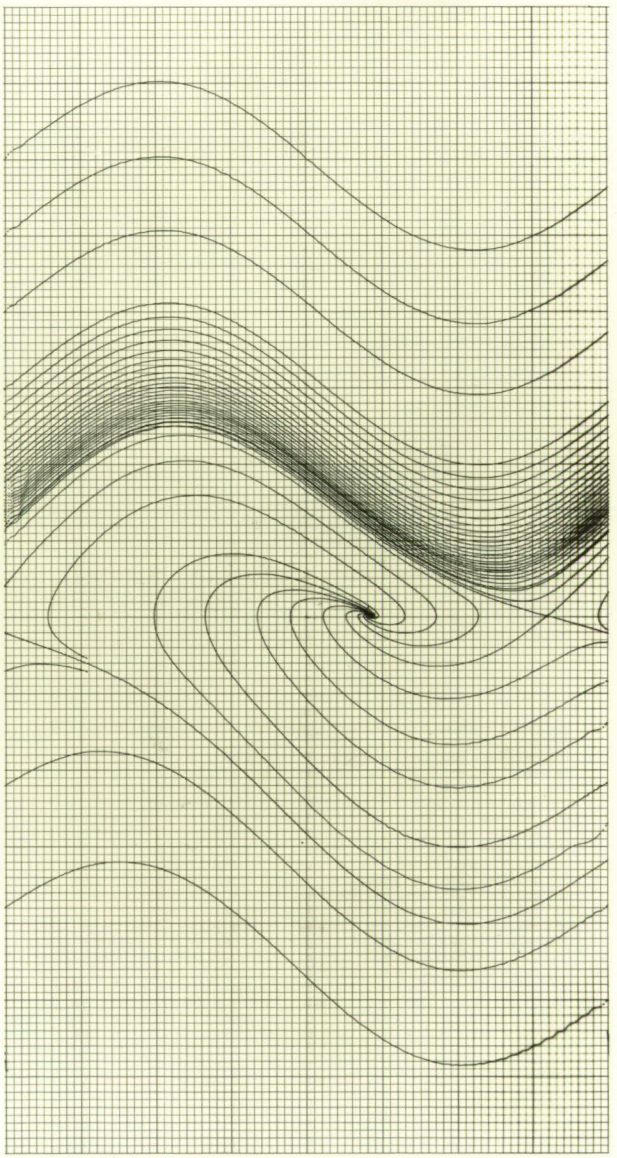

Fig. 15. $\zeta = 0.707$, $\alpha/2\zeta\omega_n = 0.1$,
$\alpha\Omega/\omega_n^2 = 0.6$, $\Omega/\omega_n = 3\sqrt{2}$

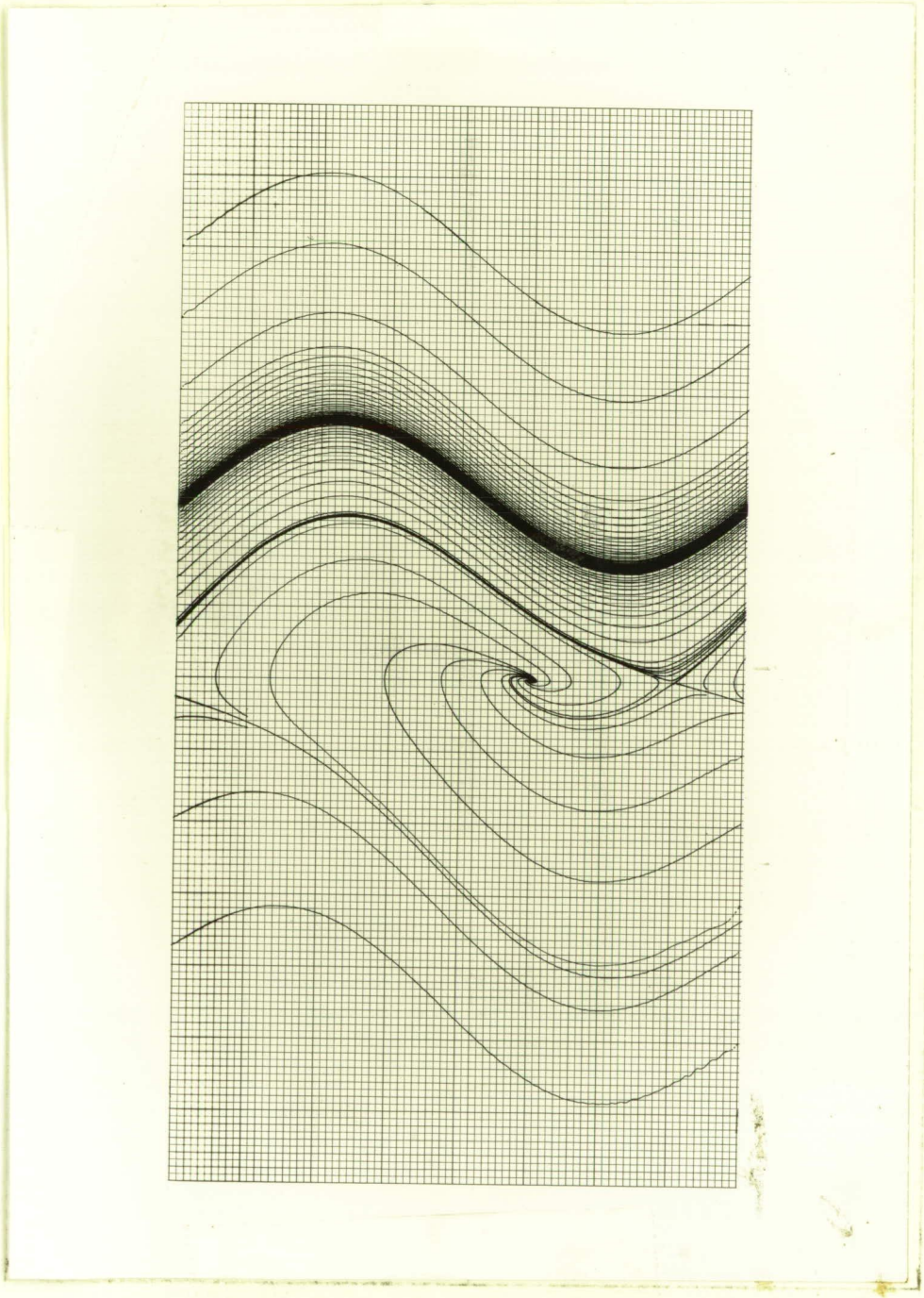

Fig. 16. $\zeta = 0.707$, $a/2\zeta\omega_n = 0.1$,
$a\Omega/\omega_n^2 = 0.7$, $\Omega/\omega_n = 7/2\sqrt{2}$

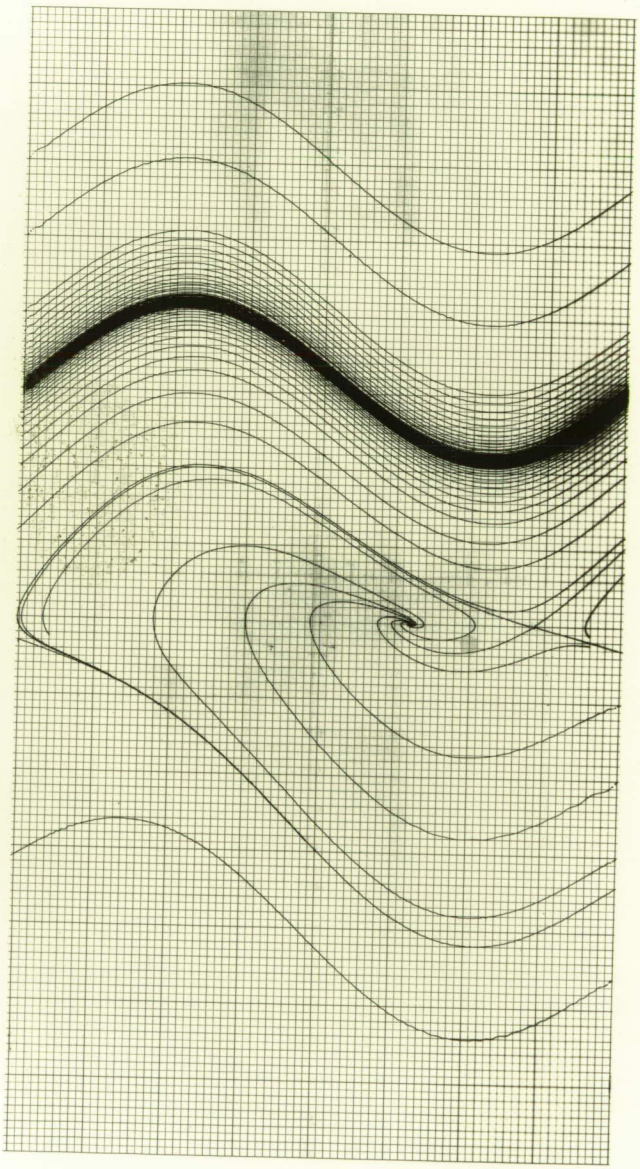

Fig. 17. $\zeta = 0.707$, $\alpha/2\zeta\omega_n = 0.1$,
$\alpha\Omega/\omega_n^2 = 0.8$, $\Omega/\omega_n = 4\sqrt{2}$

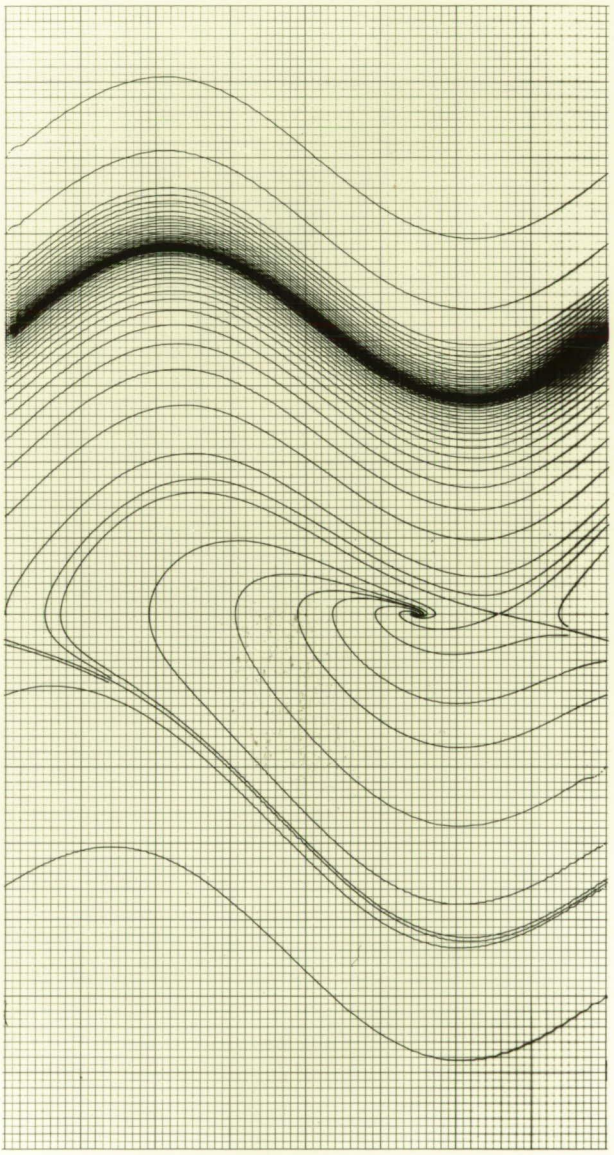

Fig. 18. $\zeta = 0.707$, $\alpha/2\zeta\omega_n = 0.1$,
$\alpha\Omega/\omega_n^2 = 0.9$, $\Omega/\omega_n = 9/2\sqrt{2}$

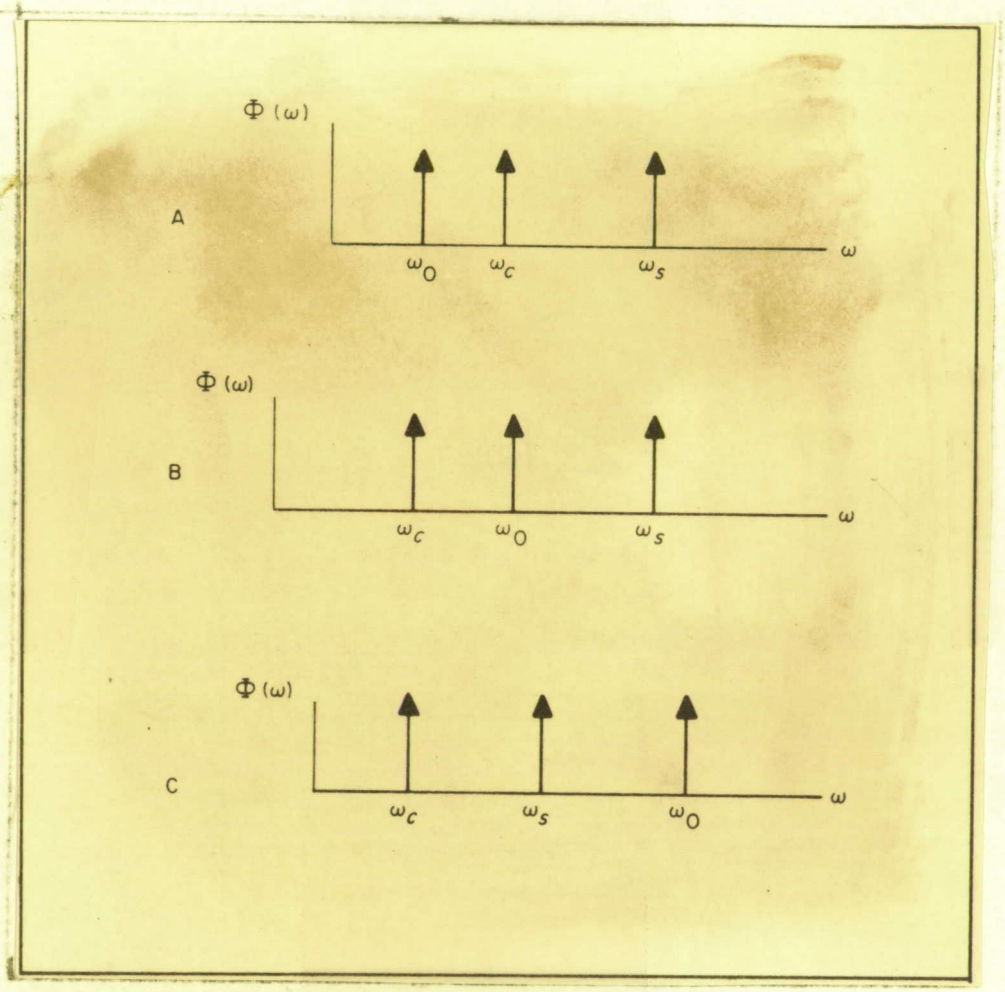

Fig. 19. Relative Positions of Signal, Center, and Initial VCO Frequencies

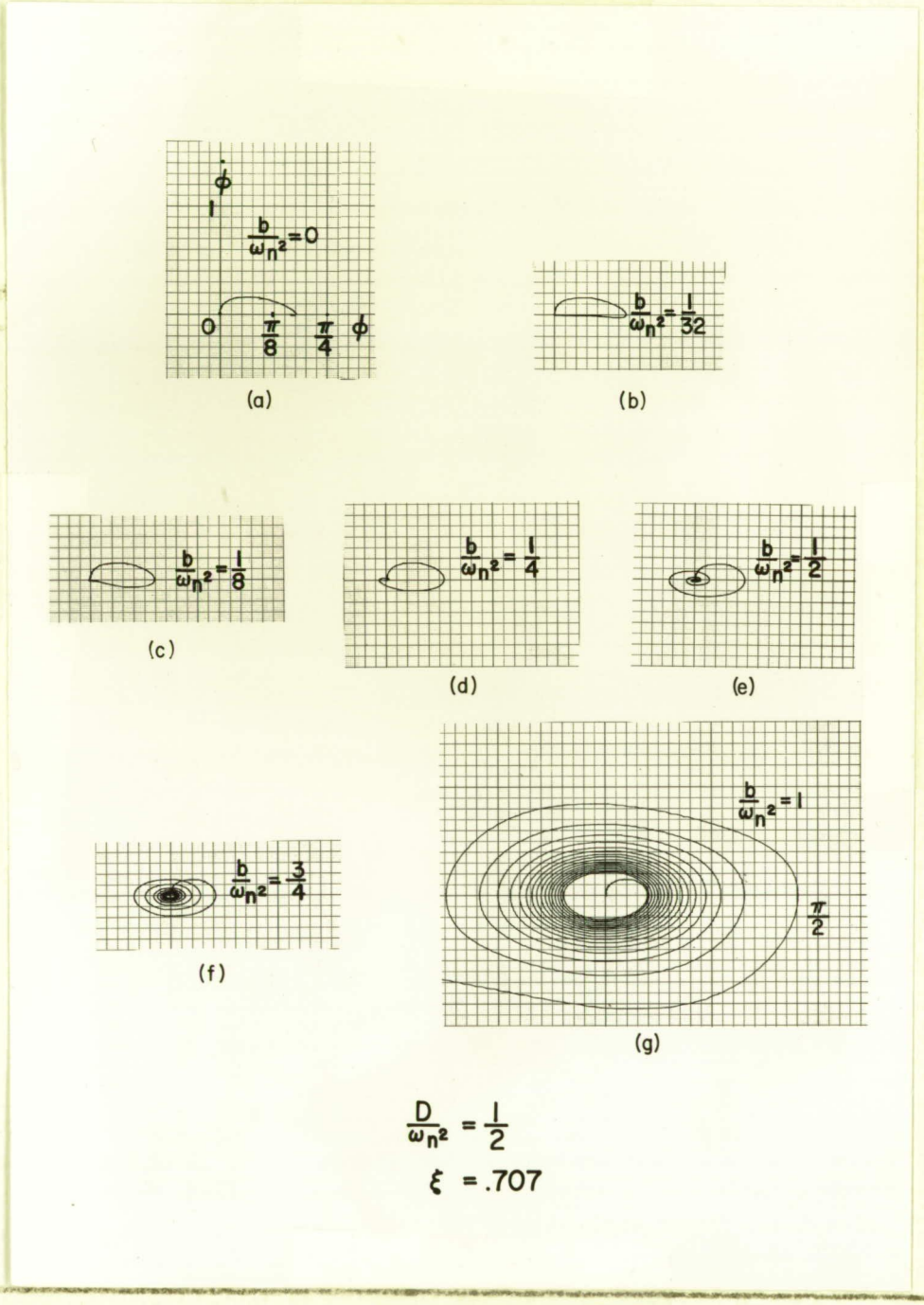

$$\frac{D}{\omega_n^2} = \frac{1}{2}$$

$$\xi = .707$$

Fig. 20. $\zeta = 0.707$, $D/\omega_n^2 = 1/2$

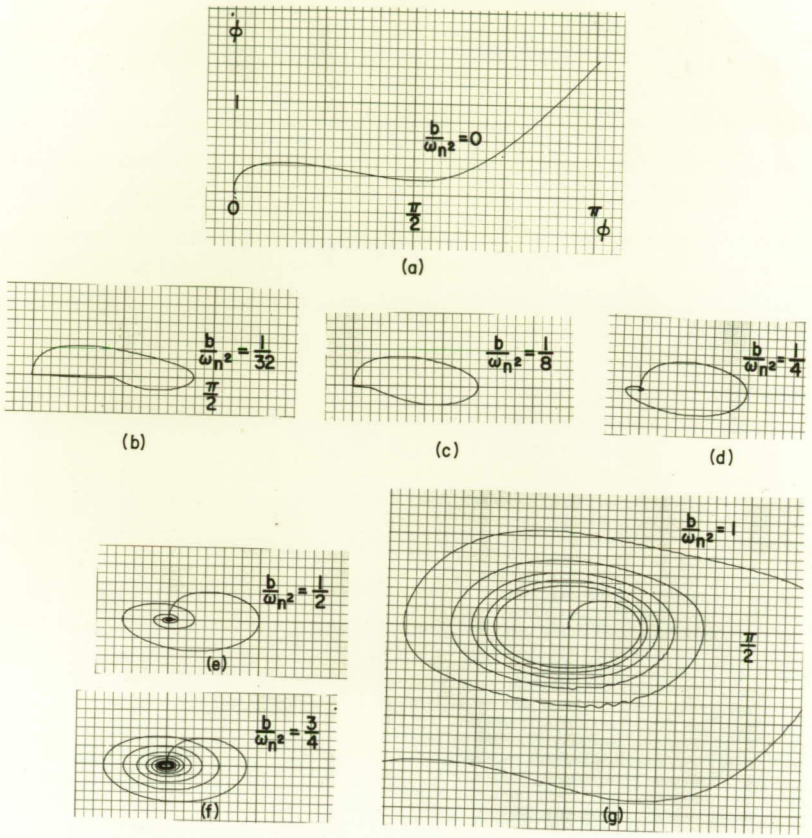

$\frac{D}{\omega_n^2}=1$

$\xi=.707$

Fig. 21. $\zeta = 0.707$, $D/\omega_n^2 = 1.0$

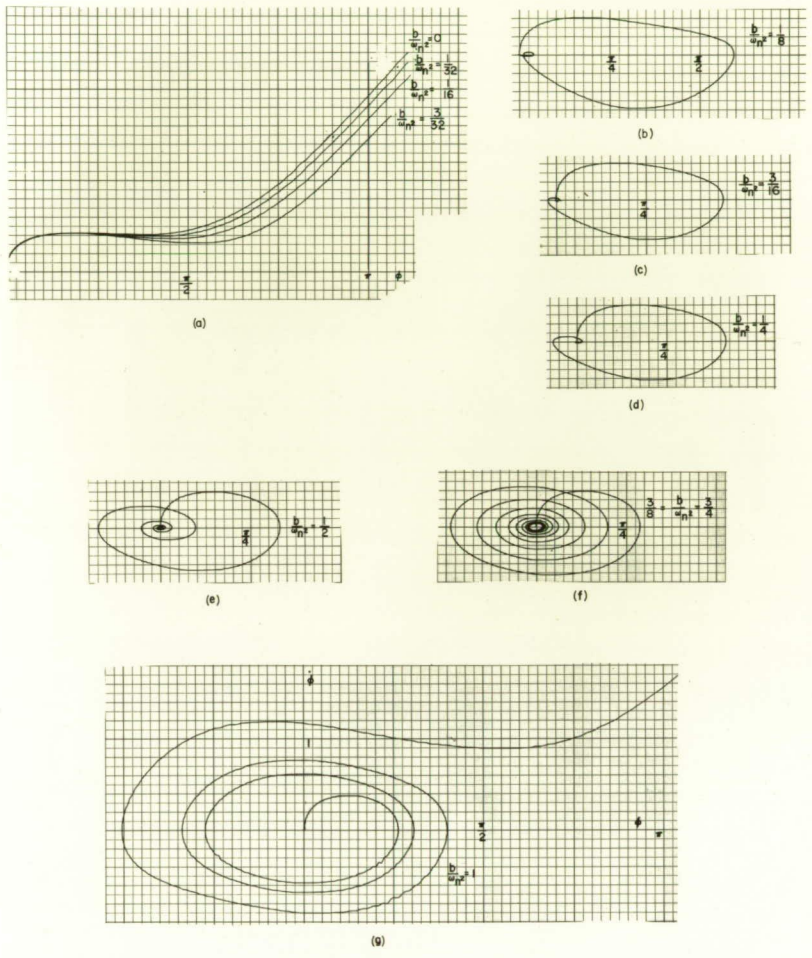

Fig. 22. $\zeta = 0.707$, $D/\omega_n^2 = 5/4$

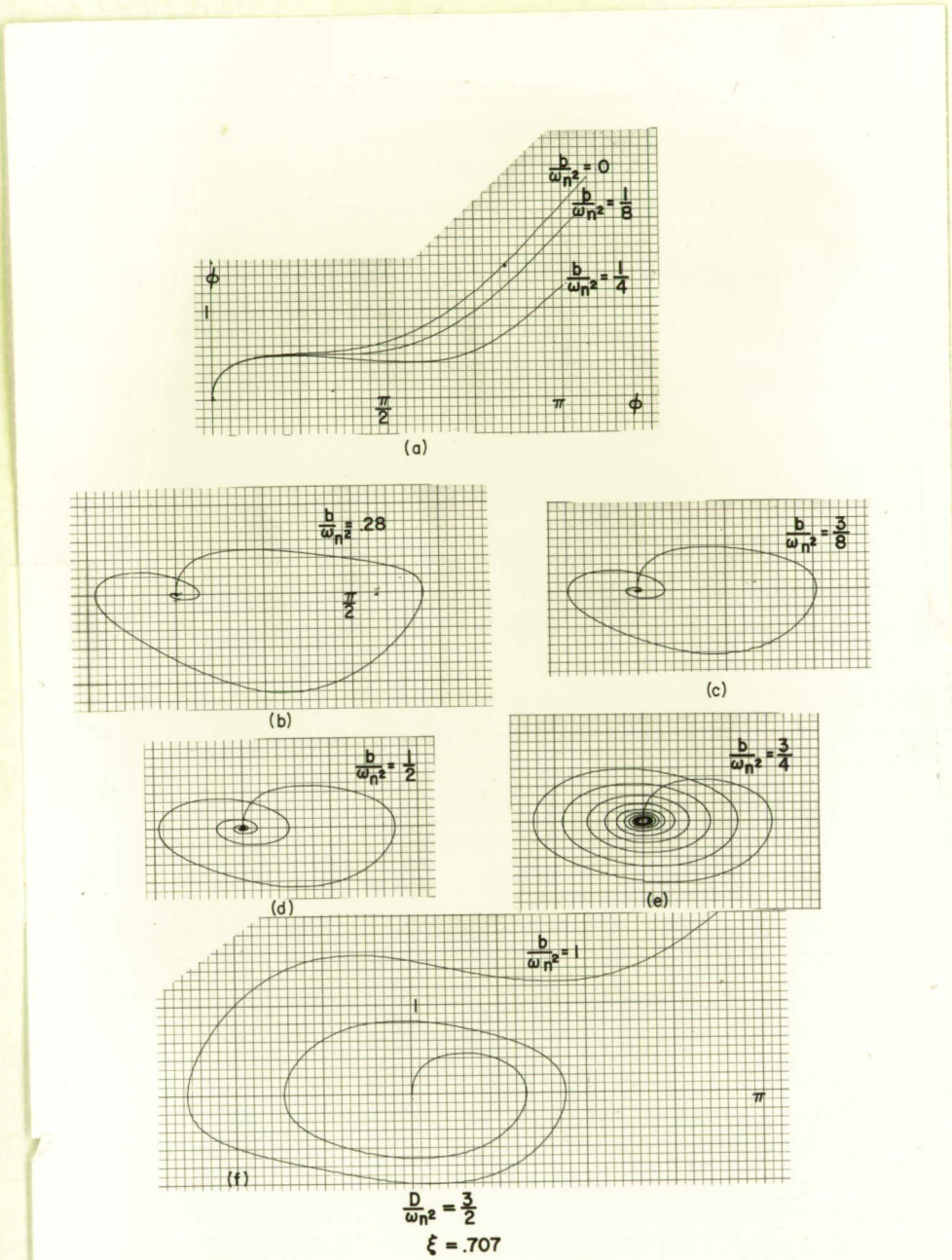

Fig. 23. $\zeta = 0.707$, $D/\omega_n^2 = 3/2$

Last line of text or footnote

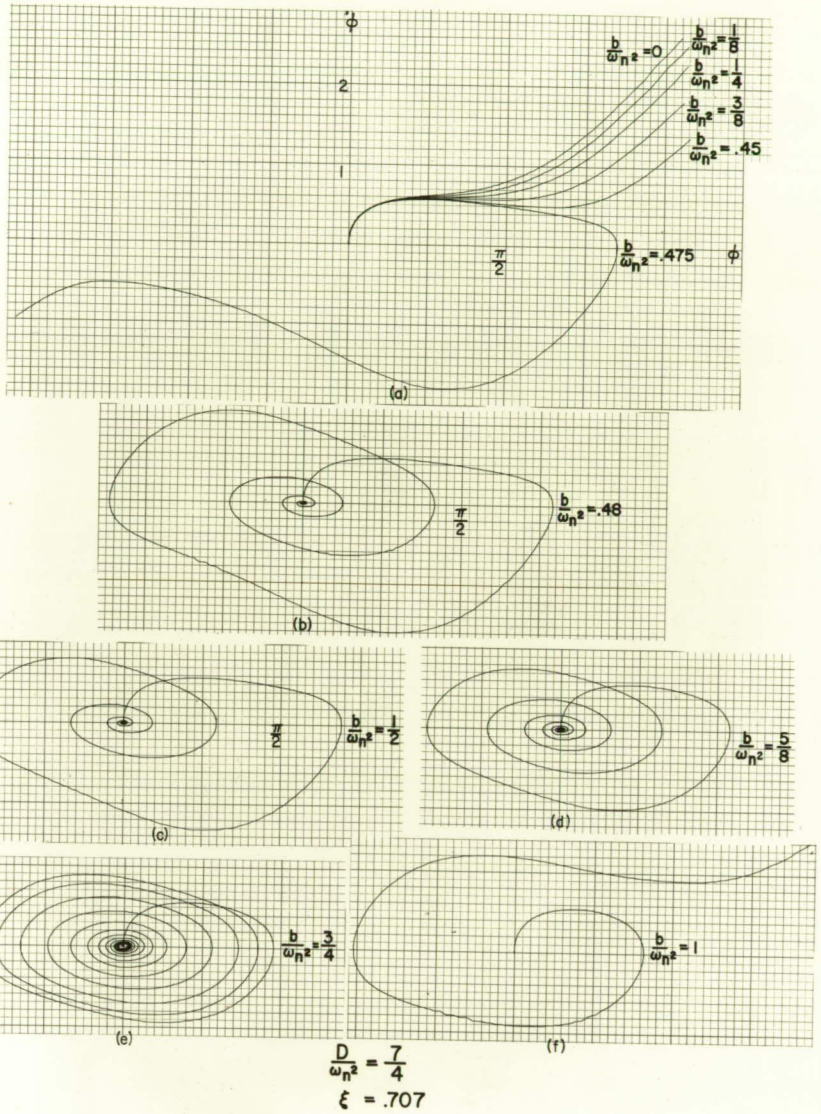

$\frac{D}{\omega_n^2} = \frac{7}{4}$

$\xi = .707$

Fig. 24. $\zeta = 0.707$, $D/\omega_n^2 = 7/4$

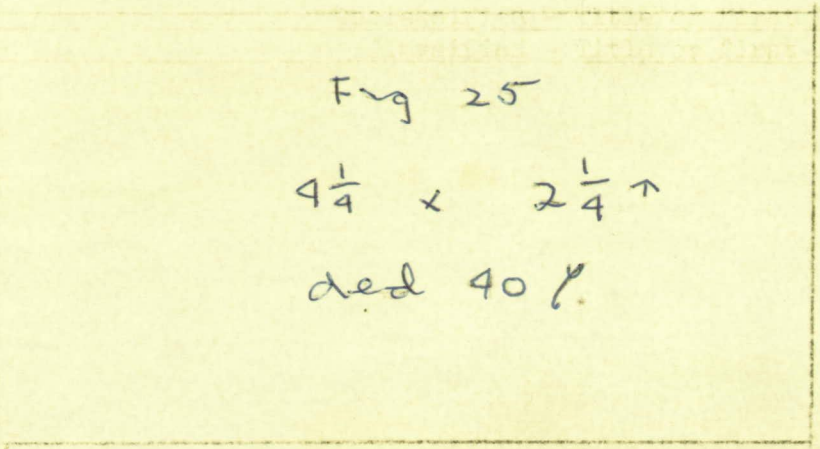

Fig. 25. $\zeta = 0.707$

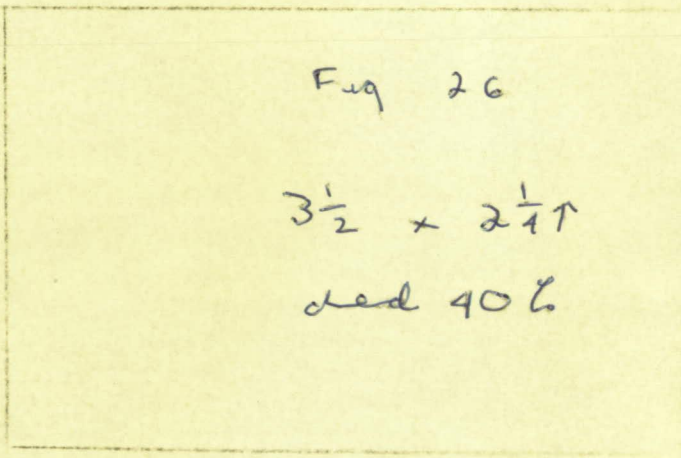

Fig. 26. $\zeta = 0.5$

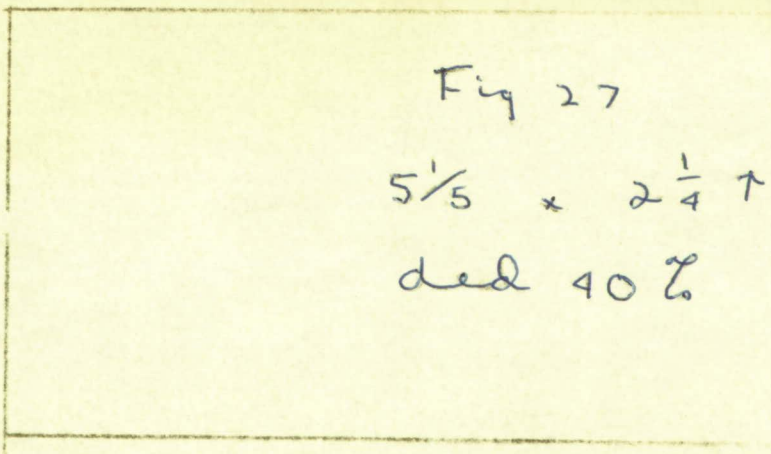

Fig. 27. $\zeta = 1.0$

ACKNOWLEDGEMENT

The author is indebted to L. R. Welch and R. C. Titsworth for their helpful suggestions and to G. A. Faist for the analog computer programs.

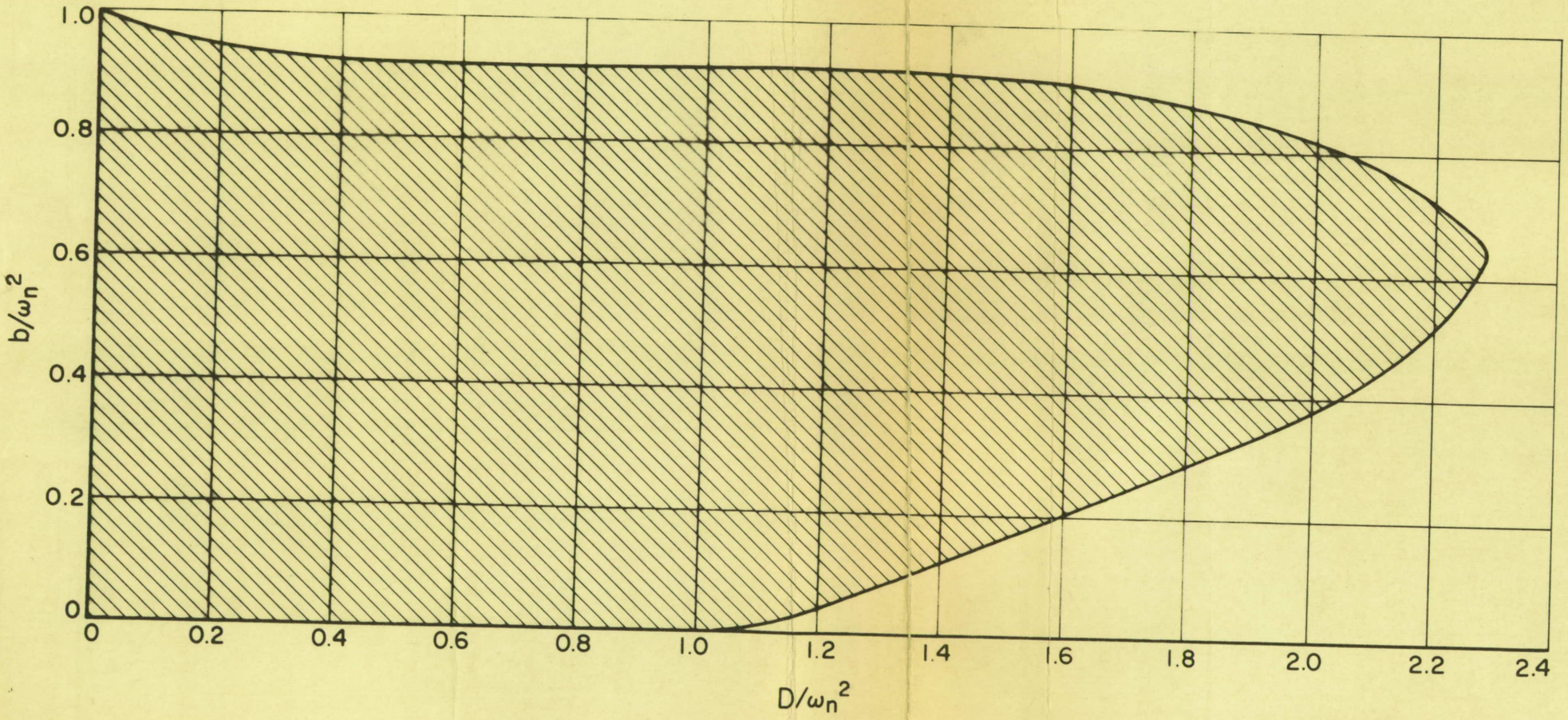
1.0
0.8
0.6
0.4
0.2
0
b/ω_n^2
0
0.2
0.4
0.6
0.8
1.0
1.2
1.4
1.6
1.8
2.0
2.2
2.4
D/ω_n^2

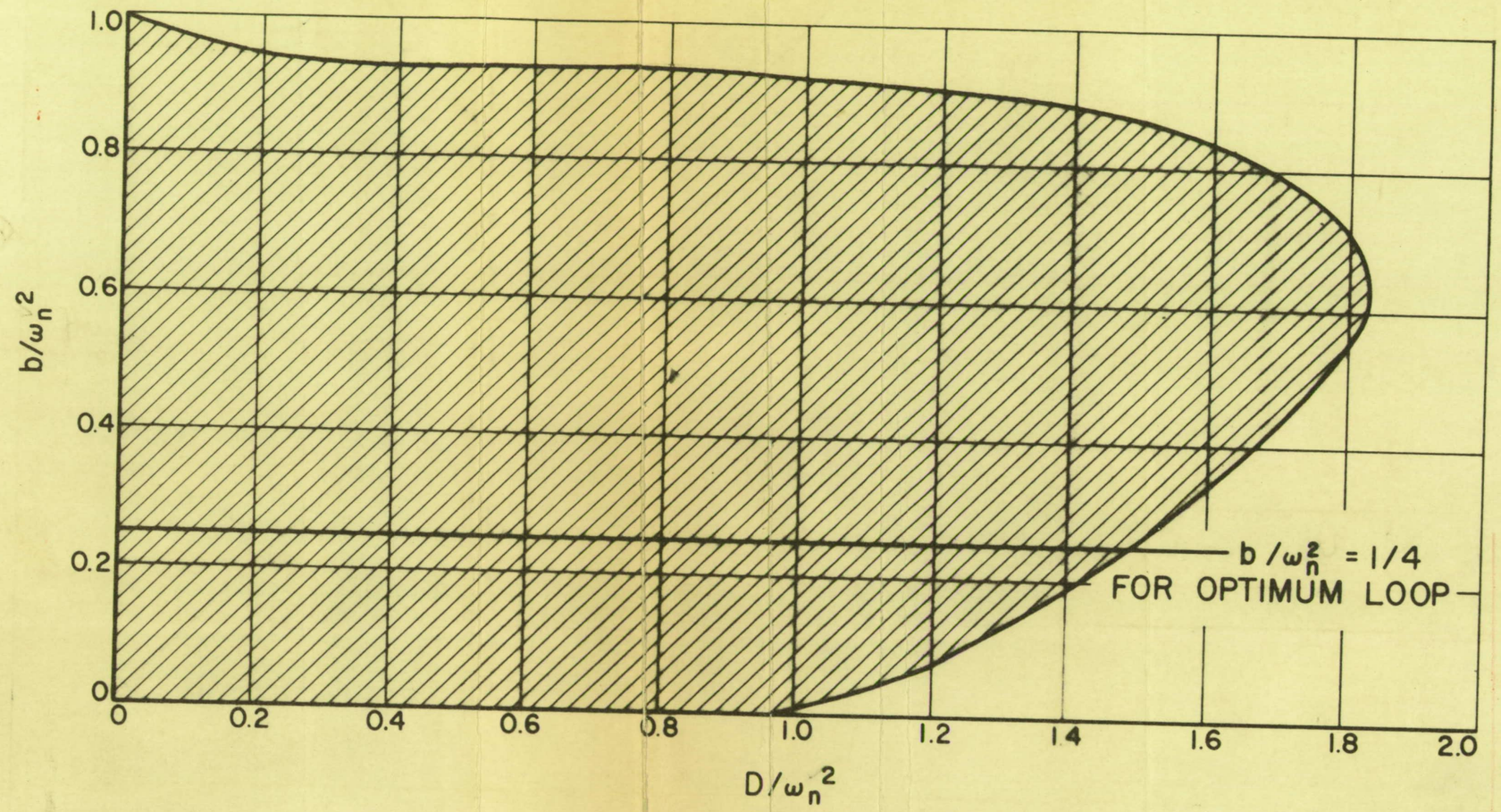

EP 673
Rpt.
Fig. 25
red. 40 %
to Rpt.
Fig.
red.
to Rpt.
Fig.
red.

Rpt. EP 673
Fig. 8
red. 78%
to Rpt.
Fig.
red.
to Rpt.
Fig.
red.

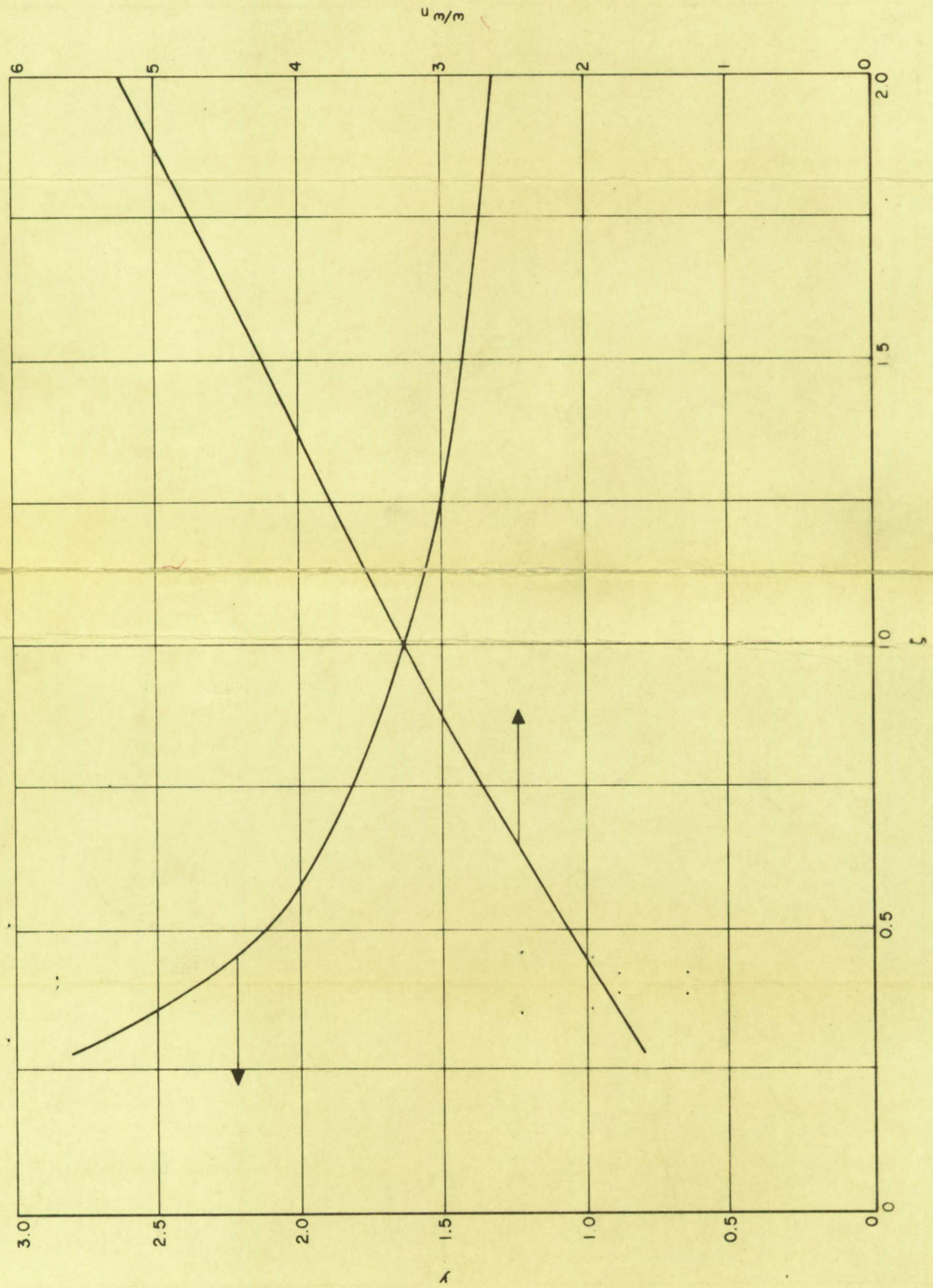

Rpt. * SP 673
Fig. 26
red. 4-6-7-
to Rpt. 7/25/39
Fig.
red.
to Rpt.
Fig.
red.

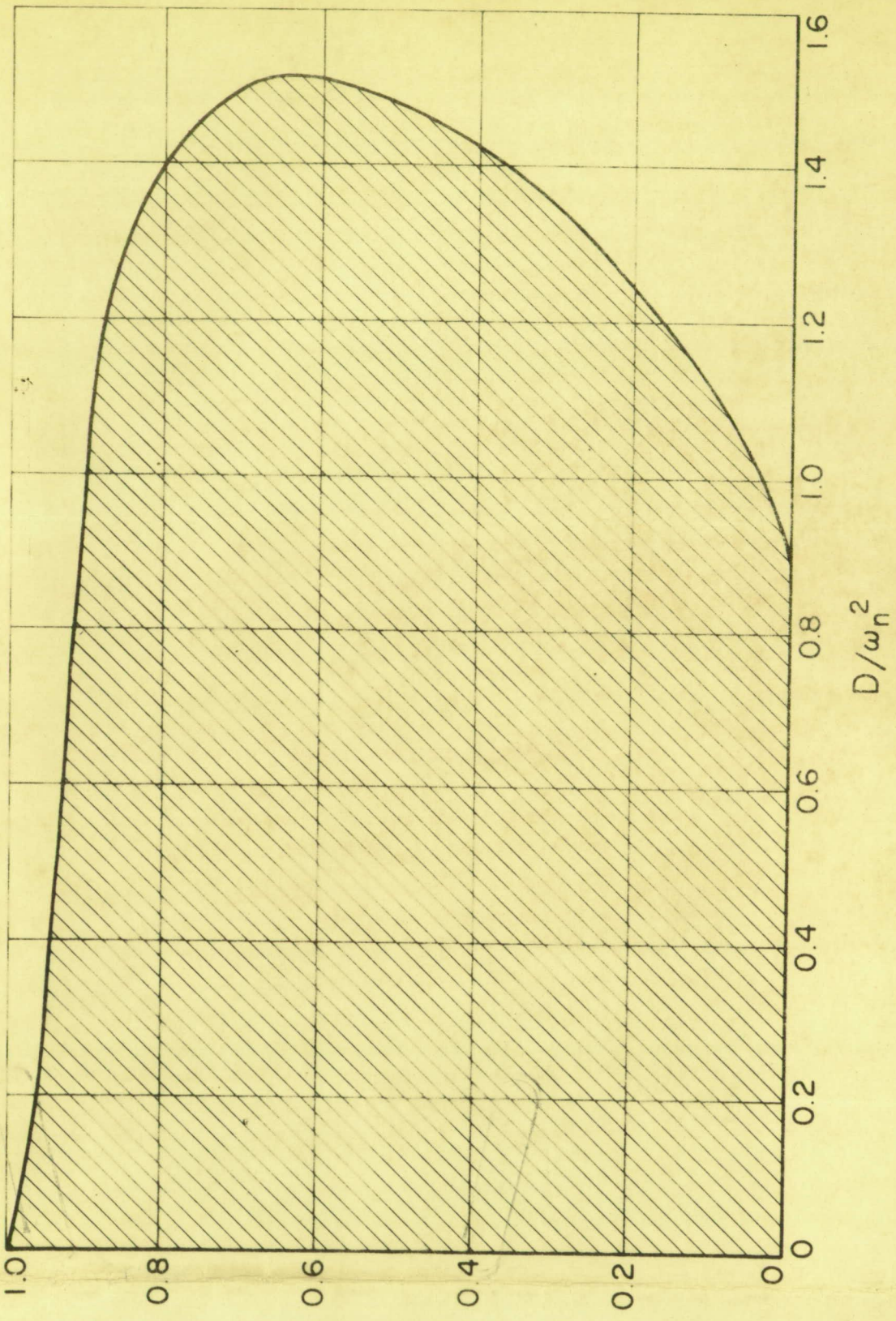

7 8 Sept 60	As_2S_3 F 254 1.1 μ 600	CsI Al	Standard	a)1.1 x 10^{-12} b)0.1	a)Al subsurface developed high resistance despite step on LiF window. b)Semiconductor on target limited to central area. c)Voltages on image section flanges: -15.00 KV, -14.3 KV, -14.1 KV. d)Flange Diameters 2.753", 2.754", 2.744", 2.761". e)To Dage 22 Sept 60, Returned 12 Dec 60, To Elmira 14 Dec 60. Window Cracked while in transport.	None	Discarded
8 19 Sept 60	As_2S_3 F 297 1.3 μ 500	CsI Pt	Standard	No Data	Image Section Tipoff Cracked during Cutoff of Tube	None	Salvage
9 26 Sept 60	As_2S_3 F 289	CsI Al	Standard	a)5.7 x 10^{-13}	Tube broke while being inserted in the vibration mount 11 Oct 60	None	Salvage
10 6 Oct 60	As_2S_3 F 333 No. 3 1.0 μ 450	CsI Pt	Standard	a)2.8 x 10^{-13} d)2.5% at 1600 A	a)Very high resistance subsurface b)Ba from getter deposited on photosurface giving visible light response. c)Tube broke while being inserted in vibration testing mount 28 Oct 60.	None	Salvage
11 26 Oct 60	As_2S_3 F 368 No. 3 1.6 μ 375	CsI Pd	Standard	No data	High resistance of subsurface - faulty manufacturing	None	Salvage
12 3 Nov 60	As_2S_3 F 368 No. 3 From tube No. 11	CsI Pd	Standard	a)1.25 x 10^{-12} b)0.1 c)13 d)2.5% at 1600 Å		Potting sample	Shipped to Dage 1 Dec 60

APPENDIX I

Uvicon Log

This appendix contains information about all of the tubes which have been fabricated during the course of this contract. Information which cannot be readily conveyed in this table is included in the following appendices.

All pretest gain measurements have been made with 50 volts on the target.

1.Tube Number Cutoff Date	2.Target a)Type b)Number c)Thickness d)Pretest gain	3.Photosurface a)Type b)Subsurface	4.Vidicon a)Type b)Number	5.Tube Performance a)Sensitivity amps/cm^2 b)Time Constant - sec c)Resolution TV lines/mm d)Quantum Yield	6.Comments	7.Suitable Application	8.Ultimate Disposition
1 18 May 60	Se	None	Standard	Not Applicable	Vibrated Laterally. Target Survived.	Mechanical Model	SAo
2 16 June 60	Se	CsI Al	Standard	No Data	Target Inserted Backwards.	None	Salvage
3 11 July 60	Se-5% P	CsI Pt	Standard	Marginal Operation	Electron Lens Tilted - Crystal Spots in Target Grew Rapidly	Electrical Model	Air Armaments Inc. 17 Aug 60
4 18 July 60	Se	CsI Pt	Standard	Marginal Operation	Tube Gassy 1 Aug 60, Window Seal Leaked Rapid Crystal Spot Growth in Target	None	Salvage
5 26 July 60	As_2S_3	CsI Pt	Standard	No Data	Tipoff Cracked on night of 26 July 60	None	Salvage
6 19 Aug 60	As_2S_3	CsI Pt	Standard	No Data	Target Broke During Processing	None	Salvage